

The Asymptotic Distribution of Sample Canonical Directions in Gaussian Spiked High-dimensional CCA

Zhangni Pu^{*1}, Zhangxiao Zhuo^{†1}, and Jiang Hu^{‡1}

¹KLASMOE, Key Laboratory of Big Data Analysis of Jilin Province and School of Mathematics & Statistics, Northeast Normal University, No. 5268 People's Street, Changchun 130024, China

Abstract

This paper studies the asymptotic behavior of sample canonical directions in a finite-rank spiked high-dimensional canonical correlation analysis model under a Gaussian population assumption. Under the asymptotic regime in which the dimensions of the two data blocks grow proportionally with the sample size, sample canonical directions are generally not consistent estimators of their population counterparts, even when the corresponding sample canonical correlations separate from the bulk spectrum. To quantify directional recovery, we investigate the squared alignment between a sample canonical direction and its associated population direction. For each simple population spike, we first establish a deterministic first-order limit for this squared alignment, which gives an explicit measure of the population-level directional information retained by the sample direction. We then prove a central limit theorem for its fluctuations around the deterministic limit, with an explicit asymptotic variance expressed through deterministic limits of resolvent trace functionals. To make the theoretical quantities computable from data, we further construct plug-in estimators for both the limiting mean and the asymptotic variance by inverting the deterministic outlier eigenvalue map, and prove their consistency. Numerical simulations and a real-data illustration support the theoretical results and demonstrate how the proposed estimators assess the recovery quality of sample canonical directions.

Keywords: Canonical correlation analysis, Random matrix theory, Spiked model, Sample canonical directions, Central limit theorem, Eigenvector alignment

1 Introduction

Canonical correlation analysis (CCA), introduced by Hotelling [13, 14], is a classical method for studying the linear association between two random vectors. Given two centered random vectors \mathbf{x} in \mathbb{R}^p and \mathbf{y} in \mathbb{R}^q , CCA seeks pairs of linear combinations whose correlations are successively maximized. In the population formulation, the squared canonical correlations and the associated

^{*}puzn687@nenu.edu.cn

[†]zhangxz722@nenu.edu.cn

[‡]hujiang156@nenu.edu.cn

canonical directions are determined by the eigenstructure of the population canonical correlation matrix

$$\Sigma_{xx}^{-1} \Sigma_{xy} \Sigma_{yy}^{-1} \Sigma_{yx}.$$

In the sample formulation, they are estimated by the eigenvalues and eigenvectors of the sample canonical correlation matrix

$$\mathbf{S}_{xx}^{-1} \mathbf{S}_{xy} \mathbf{S}_{yy}^{-1} \mathbf{S}_{yx}.$$

This eigenvalue-eigenvector representation makes CCA particularly suitable for analysis through random matrix theory.

Classical multivariate analysis studies CCA in the regime where p and q are fixed while $n \rightarrow \infty$; see, for example, [1, 21]. In many modern applications, however, the dimensions of the two data blocks are comparable to the sample size. In such high-dimensional regimes, sample canonical correlations and their associated directions exhibit behavior that is fundamentally different from classical low-dimensional asymptotics. In particular, sample canonical directions need not consistently estimate their population counterparts, even when the associated signal eigenvalues are separated from the noise bulk.

Let the columns of $(\mathbf{X}^\top, \mathbf{Y}^\top)^\top$ be n independent observations of the centered random vector $(\mathbf{x}^\top, \mathbf{y}^\top)^\top$. Denote the population covariance matrix by

$$\Sigma = \begin{pmatrix} \Sigma_{xx} & \Sigma_{xy} \\ \Sigma_{yx} & \Sigma_{yy} \end{pmatrix}.$$

The population squared canonical correlations r_i and the corresponding population canonical directions \mathbf{u}_i are determined by

$$\Sigma_{xx}^{-1} \Sigma_{xy} \Sigma_{yy}^{-1} \Sigma_{yx} \mathbf{u}_i = r_i \mathbf{u}_i.$$

The sample analogues are the eigenvalues l_i and eigenvectors $\boldsymbol{\nu}_i$ of

$$\mathbf{S}_{xx}^{-1} \mathbf{S}_{xy} \mathbf{S}_{yy}^{-1} \mathbf{S}_{yx}.$$

The main objective of this paper is to quantify, in a finite-rank spiked high-dimensional CCA model, how well a sample canonical direction $\boldsymbol{\nu}_i$ aligns with its population counterpart \mathbf{u}_i .

Throughout the theoretical analysis we work in the Gaussian spiked CCA model

$$\mathbf{X} = \mathbf{\Lambda} \mathbf{Y} + \mathbf{\Gamma} \mathbf{W}, \quad \mathbf{\Lambda} \mathbf{\Lambda}^\top + \mathbf{\Gamma} \mathbf{\Gamma}^\top = \mathbf{I}_p,$$

following the spiked CCA framework in [8]. Here \mathbf{Y} and \mathbf{W} have independent Gaussian entries. The nonzero eigenvalues of $\mathbf{\Lambda} \mathbf{\Lambda}^\top$ are the population spikes r_1, \dots, r_k . Since canonical directions are defined only up to sign, we measure directional recovery through the squared alignment

$$\langle \mathbf{u}_i, \boldsymbol{\nu}_i \rangle^2.$$

This quantity is the squared cosine of the angle between the population and sample canonical directions and is invariant under sign changes of the eigenvectors.

We work under the following dimensional assumption.

Assumption 1.1 (On the dimensions). We assume that $p := p(n)$, $q := q(n)$, and, as $n \rightarrow \infty$,

$$p/n \rightarrow c_1 \in (0, 1), \quad q/n \rightarrow c_2 \in (0, 1), \quad \text{s.t. } c_1 + c_2 \in (0, 1).$$

Without loss of generality, we always work with the additional assumption $p > q$, thus $c_1 > c_2$.

Assumption 1.2 (On the population spiked model). We assume that $\text{rank}(\mathbf{\Sigma}_{xy}) = k$ for some fixed positive integer k . Let r_i denote the i -th largest non-zero eigenvalue of the population matrix $\mathbf{\Sigma}_{xx}^{-1} \mathbf{\Sigma}_{xy} \mathbf{\Sigma}_{yy}^{-1} \mathbf{\Sigma}_{yx}$. We assume these eigenvalues are "spiked":

$$1 > r_1 \geq \dots \geq r_i \geq \dots \geq r_k > r_c := \sqrt{\frac{c_1 c_2}{(1 - c_1)(1 - c_2)}}.$$

Remark 1.3. The threshold r_c is the phase-transition threshold for sample canonical correlation matrices [8, 20]. Population spikes above this threshold produce sample eigenvalues that separate from the upper edge of the bulk limiting spectral distribution. Under Assumption 1.2, the associated sample eigenvalues are therefore sample spiked eigenvalues, and the corresponding sample eigenvectors can be studied individually.

1.1 Previous related theoretical results

We first recall the spectral theory for sample canonical correlation matrices in the high-dimensional null and spiked settings. The empirical spectral distribution (ESD)

$$F_n(x) := \frac{1}{q} \sum_{i=1}^q I(l_i \leq x)$$

converges weakly to a deterministic probability distribution $F(x)$ [24], whose density is

$$f(x) = \frac{1}{2\pi c_2} \frac{\sqrt{(d_+ - x)(x - d_-)}}{x(1 - x)} I(d_- \leq x \leq d_+), \quad (1)$$

where $d_{\pm} = (\sqrt{c_1(1 - c_2)} \pm \sqrt{c_2(1 - c_1)})^2$. Central limit theorems for linear spectral statistics and related global spectral quantities have been further developed in [28–30].

In the finite-rank setting, the sample canonical correlation matrix $\mathbf{S}_{xx}^{-1} \mathbf{S}_{xy} \mathbf{S}_{yy}^{-1} \mathbf{S}_{yx}$ can be viewed as a finite-rank perturbation of the null model. The perturbation does not change the limiting spectral distribution of the bulk, but sufficiently strong population canonical correlations generate sample outliers. Bao et al. [8] analyzed the limiting behavior and fluctuations of its largest eigenvalues in this spiked setting. Let

$$\gamma_i := r_i(1 - c_1 + c_1 r_i^{-1})(1 - c_2 + c_2 r_i^{-1}). \quad (2)$$

Theorem 1.4 (Theorem 1.7 of [8]). *Under Assumptions 1.1 and 1.2, the squares of the sample canonical coefficients exhibit the following convergence:*

1. (*Outliers*) For $1 \leq i \leq k$, as $n \rightarrow \infty$, we have $l_i - \gamma_i \xrightarrow{\text{a.s.}} 0$.

2. (*Sticking eigenvalues*) For each fixed $i \geq k + 1$, as $n \rightarrow \infty$, we have $l_i - d_+ \xrightarrow{a.s.} 0$.

Extensions of the spiked CCA eigenvalue theory to non-Gaussian populations and related Fisher-type models have been studied in [3, 15, 20, 27]. These eigenvalue results provide the spectral foundation for signal detection in high-dimensional CCA. However, eigenvalue separation alone does not quantify directional recovery. A separated sample canonical correlation indicates that a signal is detectable from the spectrum, but it does not describe how accurately the associated sample canonical direction estimates the corresponding population direction. This distinction motivates the eigenvector analysis developed in this paper.

The study of eigenvectors in random matrix theory (RMT) is generally more challenging than that of eigenvalues. Global-level results have investigated eigenvector empirical spectral distributions (VESD) and related quantities [4, 17, 25, 26]. Local-level studies, which are close to the goal of this paper, characterize the "distance" or "alignment" between an individual sample eigenvector and a fixed population direction. Such phenomena have been studied for spiked sample covariance matrices [6, 22, 23], deformed Wigner matrices [9, 11, 16], and information-plus-noise models [7, 18]. These works show that the squared inner product between a sample eigenvector and its population counterpart is a natural measure of directional recovery.

For high-dimensional CCA, the eigenvector problem remains less developed. Bykhovskaya and Gorin [10] study the high-dimensional behavior of canonical variables, or canonical variates, and obtain first-order limits for angles between sample and population canonical variables such as $\mathbf{X}^\top \boldsymbol{\nu}_i$, $\mathbf{X}^\top \mathbf{u}_i$. These angles are defined in the sample space. They are different from the alignment between the canonical direction vectors themselves, namely the eigenvectors and their population counterparts in the original variable spaces. The latter quantity is sensitive to the covariance structure and coordinate normalization. In particular, an asymptotic theory for the squared alignment $\langle \mathbf{u}_i, \boldsymbol{\nu}_i \rangle^2$ in a finite-rank spiked CCA model does not seem to be available in the existing literature.

1.2 Contributions and Overview of Results

This paper develops a first- and second-order asymptotic theory for sample canonical directions associated with finite-rank population spikes in high-dimensional CCA under Gaussian assumptions. Our object of interest is the squared alignment

$$\langle \mathbf{u}_i, \boldsymbol{\nu}_i \rangle^2,$$

which measures the amount of population-level directional information retained by the sample canonical direction.

Our first contribution is a deterministic first-order characterization of this squared alignment. For each simple spike r_i , we prove that

$$\langle \mathbf{u}_i, \boldsymbol{\nu}_i \rangle^2 \xrightarrow{p} \frac{1}{1 + d(r_i)},$$

where $d(r_i)$ is an explicit function of the population spike r_i and c_1, c_2 . The limit is generally strictly smaller than one. Thus, the sample canonical direction is not classically consistent in the high-dimensional regime. At the same time, the result gives an explicit limiting measure of

the recovery quality of the sample direction. Similar non-consistency phenomena and nontrivial eigenvector alignment limits have appeared in other spiked random matrix models, including spiked sample covariance matrices [6, 22, 23], deformed Wigner matrices [11], and information-plus-noise matrices [7, 18].

Our main contribution is a CLT for the fluctuation of the squared alignment. Specifically, we show that

$$\sqrt{n} \left(\langle \mathbf{u}_i, \mathbf{v}_i \rangle^2 - \frac{1}{1 + d(r_i)} \right)$$

converges in distribution to a centered normal distribution with variance $\sigma^2(r_i)/(1 + d(r_i))^4$. Here $\sigma(r_i)^2$ is given explicitly in terms of deterministic limits of resolvent trace functionals. To the best of our knowledge, this is the first CLT for the squared alignment between a sample canonical direction and its population counterpart in the finite-rank spiked high-dimensional CCA model. This result upgrades the directional recovery theory from a deterministic approximation to a distributional approximation.

Our third contribution is to make the preceding asymptotic quantities estimable from data. Since both the limiting mean and the asymptotic variance depend on the unknown population spike r_i , we estimate r_i through the deterministic outlier map

$$\hat{r}_i = \gamma^{-1}(l_i).$$

Substituting \hat{r}_i into the deterministic expressions yields plug-in estimators

$$\hat{\mu}_i = \frac{1}{1 + d(\hat{r}_i)} \quad \text{and} \quad \hat{\sigma}_i^2 = \frac{\sigma^2(\hat{r}_i)}{(1 + d(\hat{r}_i))^4}.$$

We prove that these estimators consistently estimate the limiting mean and asymptotic variance of the squared alignment, respectively. Consequently, the theory provides a sample-based measure of both the strength and the uncertainty of directional recovery.

On the technical side, our proof is based on a detailed analysis of the characteristic equation for the sample canonical correlation matrix. By applying the Schur complement, the eigenvector problem is reduced to the study of a finite-dimensional random matrix involving resolvents of the noise part of the CCA matrix. This reduction expresses the normalization of the sample eigenvector in terms of finite-dimensional random matrices involving resolvents of the noise part of the model. We then derive deterministic equivalents and fluctuation estimates for the resulting resolvent trace functionals. The Gaussian assumption allows us to use the Gaussian Poincaré inequality and Stein's lemma, or equivalently the Gaussian cumulant expansion, to control variances and compute the limiting covariance structure.

Finally, we provide numerical illustrations to support the theoretical results. The simulation study illustrates the first-order deterministic limit and the Gaussian fluctuation in rank-one and multi-spike settings. We also present a real-data illustration using the limestone grassland community data originally reported by Gittins [12] and also analyzed in Bao et al. [8]. In this example, the leading sample squared canonical correlation separates from the bulk, and the plug-in estimate $\hat{\mu}_1$ provides a quantitative assessment of the recovery quality of the leading sample canonical direction. This illustrates how the proposed theory can be used to interpret

sample canonical directions when the corresponding population directions are unobservable.

1.3 Organization and notation

The remainder of the paper is organized as follows. Section 2 presents the preliminary technical lemmas and our main theoretical results, including the first-order limit and the central limit theorem for the squared alignment. Section 3 constructs plug-in estimators for the limiting mean and asymptotic variance of the squared alignment and presents a real-data illustration. Section 4 reports Monte Carlo simulations supporting the theoretical results. Section 5 proves the main theorems, while the remaining sections provide the required technical estimates.

Throughout the paper, $\|\cdot\|$ denotes the Euclidean norm for vectors and the operator norm for matrices. For a matrix \mathbf{A} , $\text{tr}\mathbf{A}$ denotes its trace, and \mathbf{A}^\top denotes its transpose. We write \xrightarrow{p} , $\xrightarrow{a.s.}$, and \xrightarrow{D} for convergence in probability, almost sure convergence, and convergence in distribution, respectively.

2 Main Results

In this section, we state our main results and introduce the necessary technical lemmas that support our proofs and calculations in the subsequent sections.

2.1 Preliminary Technical Lemmas

We begin with several standard definitions and results that are fundamental to our analysis.

Definition 2.1. Let ξ_n be a sequence of random variables and $\{C_n\}$ be a sequence of positive constants. We say $\xi_n = O_p(C_n)$ if for all $\varepsilon > 0$, there exist constants N_ε and K_ε such that for all $n > N_\varepsilon$, $\mathbb{P}(|\xi_n/C_n| \leq K_\varepsilon) \geq 1 - \varepsilon$.

Note that if $\sup_n \mathbb{E}|\xi_n|^l < \infty$ for some $l \geq 1$, then $\xi_n = O_p(1)$ by Markov's inequality. The following cumulant expansion formula plays a central role in our computation, with a proof found in [19].

Lemma 2.2 (Cumulant expansion formula). *Let $f : \mathbb{R} \rightarrow \mathbb{C}$ be a smooth function, and denote by $f^{(k)}$ its k th derivative. Then for every fixed $l \in \mathbb{N}$, we have*

$$\mathbb{E}[\xi f(\xi)] = \sum_{k=0}^l \frac{\kappa_{k+1}(\xi)}{k!} \mathbb{E}[f^{(k)}(\xi)] + \mathcal{R}_{l+1}, \quad (3)$$

assuming that all expectations in (3) exist, where \mathcal{R}_{l+1} is the remainder term (depending on f and ξ), such that for any $t > 0$,

$$\mathcal{R}_{l+1} = O(1)\mathbb{E}[|\xi|^{l+2}I_{|\xi| > t}] \sup_{x \in \mathbb{R}} |f^{(l+1)}(x)| + O(1)\mathbb{E}[|\xi|^{l+2}] \sup_{|x| \leq t} |f^{(l+1)}(x)|.$$

In particular, if ξ is from a standard normal distribution, $\kappa_1(\xi) = 0$, $\kappa_2(\xi) = 1$, and $\kappa_j(\xi) = 0$ for $j \geq 3$. We then get the famous Stein's Lemma:

$$\mathbb{E}[\xi f(\xi)] = \mathbb{E}[f'(\xi)]. \quad (4)$$

Lemma 2.3 (Gaussian Poincaré inequality). *Let μ be the standard Gaussian measure on $M = \mathbb{R}^n$. Assume $f : \mathbb{R}^n \rightarrow \mathbb{R}$ is C^1 . Then, $\text{Var}_\mu(f) \leq C \mathbb{E}_\mu |\nabla f|^2$ holds with $C = 1$. In particular, let $\{\xi_i\}_{i=1}^n$ with standard normal distribution be independent, and assume the function $f : \mathbb{R}^n \rightarrow \mathbb{R}$ has first-order continuous partial derivatives. Then we have*

$$\text{Var}[f(\xi_1, \dots, \xi_n)] \leq \mathbb{E} \sum_{i=1}^n \left[\frac{\partial f(\xi_1, \dots, \xi_n)}{\partial \xi_i} \right]^2.$$

2.2 Asymptotic Results for the Squared Alignment

Under the model $\mathbf{X} = \mathbf{\Lambda Y} + \mathbf{\Gamma W}$, the finite-rank population correlation structure is encoded in $\mathbf{\Lambda}$. Since the population and sample canonical directions are defined only up to sign and are normalized to have unit norm, we study the squared inner product between them. The squared inner product $\langle \mathbf{u}_i, \boldsymbol{\nu}_i \rangle^2$ is the squared cosine of the angle between the population and sample canonical directions. The first-order approximation of the squared cosine of this angle is given below.

Theorem 2.4 (First-order limit). *Under Assumptions 1.1-1.2, fix $1 \leq i \leq k$ such that r_i is a simple spike. Then*

$$\langle \mathbf{u}_i, \boldsymbol{\nu}_i \rangle^2 \xrightarrow{p} \frac{1}{1 + d(r_i)}, \quad (5)$$

where $d(r_i) = D_1(r_i) + D_2(r_i)$, and

$$\begin{aligned} D_1(r_i) &= (1 - r_i) \left(\frac{2(\eta r_i - \omega)(1 - r_i) - r_i}{r_i} F_1(r_i) \right. \\ &\quad \left. + \frac{r_i(\eta r_i - \omega)(1 - r_i) - (\eta r_i - \omega)^2(1 - r_i)^2}{r_i^2} F_2(r_i) \right), \\ D_2(r_i) &= \frac{r_i(\eta r_i - \omega)^2(1 - r_i)^2}{c_2 r_i^2} \left(\left(\frac{c_1 r_i + \omega(1 - r_i)}{r_i - (\eta r_i - \omega)(1 - r_i)} - \frac{\omega}{\eta r_i - \omega} \right) F_1(r_i) \right. \\ &\quad \left. + \left(c_1 + c_2 - \frac{2\omega(1 - r_i)}{r_i} \right) F_2(r_i) \right), \\ F_1(r_i) &= \frac{-c_1 r_i((1 - c_2)r_i + c_2)}{r_i(\eta r_i - \omega) - (\eta r_i - \omega)^2(1 - r_i)}, \\ F_2(r_i) &= \frac{r_i^2 (\omega(1 - c_2)r_i((1 - c_1)r_i + c_1) + c_1(\eta r_i - \omega)(\eta r_i^2 - \omega))}{((1 - c_1)r_i + c_1)^2 ((1 - c_2)r_i + c_2)(\eta r_i - \omega)^2(\eta r_i^2 - \omega)}, \end{aligned}$$

with $\eta = (1 - c_1)(1 - c_2)$ and $\omega = c_1 c_2$.

Theorem 2.4 shows that the squared inner product has a deterministic limit, which implies that the sample spiked eigenvector $\boldsymbol{\nu}_i$ is asymptotically inconsistent, lying on a cone around the true population spiked eigenvector \mathbf{u}_i . Similar behavior has been observed in several spiked random matrix models, including spiked sample covariance matrices [6, 22, 23], deformed Wigner matrices [11], and information-plus-noise matrices [7, 18]. We next study the fluctuations of the squared alignment around this first-order limit. This leads to the following central limit theorem.

Theorem 2.5 (Central limit theorem). *Under the same assumptions as in Theorem 2.4, for the same simple spike r_i , the following convergence in distribution holds:*

$$\sqrt{n} \left(\langle \mathbf{u}_i, \boldsymbol{\nu}_i \rangle^2 - \frac{1}{1 + d(r_i)} \right) \xrightarrow{D} \mathcal{N}(0, \sigma^2(r_i)/(1 + d(r_i))^4), \quad (6)$$

where

$$\begin{aligned} \sigma^2(r_i) = & 2(1 - r_i)^2 P_1(r_i) - 4 \frac{\eta r_i - \omega}{r_i} (1 - r_i)^3 (P_1(r_i) + F_3(r_i)) \\ & + \frac{2(\eta r_i - \omega)^2}{r_i^2} (1 - r_i)^4 (P_1(r_i) + 2F_3(r_i) + Q_3(r_i)) \\ & + \frac{2(\eta r_i - \omega)^4 (1 - r_i)^4}{r_i^2} (J_{k1}(r_i) + J_{k2}(r_i) + J_{k3}(r_i) + J_{k4}(r_i) + J_{k5}(r_i)) \\ & + \frac{4(\eta r_i - \omega)^3 (1 - r_i)^4 Q_4(r_i)}{c_2 r_i^2} + \frac{4c_1 (\eta r_i - \omega)^2 (1 - r_i)^3 Q_7(r_i)}{c_2 r_i}. \end{aligned} \quad (7)$$

$$(8)$$

The deterministic quantities $P_1(r_i)$, $F_3(r_i)$, $Q_3(r_i)$, $J_{k\ell}(r_i)$, $\ell = 1, \dots, 5$, $Q_4(r_i)$, and $Q_7(r_i)$ are defined in (24), (36), (37), (31) – (35), (38), and (40), respectively.

Remark 2.6. To the best of our knowledge, Theorem 2.5 is the first central limit theorem for the squared alignment $\langle \mathbf{u}_i, \boldsymbol{\nu}_i \rangle^2$ in high-dimensional CCA with finite-rank population spikes. This result is proved under Assumptions 1.1–1.2, for a fixed number of spikes and for a simple spike in the separated, supercritical regime. Critical or near-critical spikes, multiple spikes with the same limiting location, and possible interactions among several spikes are not considered here.

3 Estimation of the Asymptotic Mean and Variance of the Squared Alignment

In the previous section, we show that, for each simple spike r_i , the squared alignment

$$\langle \mathbf{u}_i, \boldsymbol{\nu}_i \rangle^2$$

does not converge to one. Instead, it converges to a nontrivial limit that is strictly smaller than one. Moreover, the fluctuation around this limit occurs on the $n^{-1/2}$ scale and admits an asymptotically Gaussian description. Thus, under the high-dimensional regime considered in this paper, the sample canonical direction is not a classically consistent estimator of the population canonical direction. Instead, its squared alignment with the population direction has a nontrivial limiting value.

This suggests that, in the present setting, the relevant question is not whether the sample canonical direction fully recovers the population one, but how large the limiting squared alignment is and how it fluctuates around its limit. Theorem 2.4 identifies the asymptotic center of this alignment, while Theorem 2.5 characterizes its second-order fluctuation. However, both quantities depend on the population spike r_i , and are therefore not directly computable from data. The purpose of this section is to construct plug-in estimators for these quantities based

on the sample spiked eigenvalue l_i , thereby turning the asymptotic results of Theorems 2.4 and 2.5 into quantities that can be evaluated from the observed sample. In this sense, eigenvalue separation and directional recovery represent two different aspects of the problem. A sample spiked eigenvalue indicates that a signal direction is detectable from the spectrum, whereas the squared alignment quantifies how accurately the associated sample direction represents its population counterpart. The estimators constructed below are designed to assess this directional recovery.

3.1 Estimation of the Asymptotic Mean

By Theorem 1.4, for each sample spiked eigenvalue associated with a population spike r_i , we have

$$l_i - \gamma_i \xrightarrow{a.s.} 0, \quad \gamma_i = \gamma(r_i),$$

where $\gamma(\cdot)$ is the deterministic mapping from the population spike r_i to its associated outlier location. On the other hand, Theorem 2.4 shows that

$$\langle \mathbf{u}_i, \boldsymbol{\nu}_i \rangle^2 \xrightarrow{p} \mu_i, \quad \mu_i := \frac{1}{1 + d(r_i)}.$$

Accordingly, μ_i describes the limiting mean of the squared alignment between the sample and population canonical directions. Since μ_i depends on the unknown spike r_i , a natural strategy is to estimate r_i from the observed spiked eigenvalue l_i , and then substitute the resulting estimator into the expression for μ_i .

Proposition 3.1. *Suppose the assumptions of Theorem 1.4 and 2.4 hold, and fix a simple spike r_i . Assume that the function $\gamma(\cdot)$ is locally one-to-one in a neighborhood of r_i , and that $d(\cdot)$ is continuous at r_i . Denote by $\gamma^{-1}(\cdot)$ the corresponding local inverse on a neighborhood of $\gamma(r_i)$. Define*

$$\hat{r}_i := \gamma^{-1}(l_i), \quad \hat{\mu}_i := \frac{1}{1 + d(\hat{r}_i)}.$$

Then

$$\hat{r}_i \xrightarrow{p} r_i, \quad \hat{\mu}_i \xrightarrow{p} \mu_i.$$

The proof is postponed to Section 8.

The construction in Proposition 3.1 can be summarized as the following plug-in procedure.

Remark 3.2. The role of Proposition 3.1 is not to estimate the population direction \mathbf{u}_i itself, but to estimate the limiting mean μ_i appearing in Theorem 2.4. Since μ_i is precisely the limit of the squared alignment $\langle \mathbf{u}_i, \boldsymbol{\nu}_i \rangle^2$, it may be interpreted as the limiting mean of the squared alignment between the sample and population directions. Proposition 3.1 shows that this quantity can be consistently estimated from the observed sample spiked eigenvalue. Thus, $\hat{\mu}_i$ provides a sample-based measure of recovery quality for a direction that is itself not consistently estimable.

Table 1: Plug-in procedure for estimating the limiting mean μ_i .

Step	Procedure
1	<p>Given the centered data matrices $\mathbf{X} \in \mathbb{R}^{p \times n}$ and $\mathbf{Y} \in \mathbb{R}^{q \times n}$, form the sample canonical correlation matrix</p> $\mathbf{S}_{xx}^{-1} \mathbf{S}_{xy} \mathbf{S}_{yy}^{-1} \mathbf{S}_{yx}.$ <p>Compute its nonzero eigenvalues $l_1 \geq l_2 \geq \dots \geq l_q$.</p>
2	<p>Identify the sample spiked eigenvalues. In practice, retain those l_i satisfying</p> $l_i > d_+,$ <p>or, more conservatively, $l_i > d_+ + \varepsilon_n$, where $\varepsilon_n \downarrow 0$ is a deterministic sequence chosen to separate sample outliers from the bulk edge.</p>
3	<p>For each retained sample spiked eigenvalue l_i, estimate the corresponding population spike by</p> $\hat{r}_i = \gamma^{-1}(l_i) = \frac{2c_1 c_2 - c_1 - c_2 + l_i + \sqrt{(l_i - d_-)(l_i - d_+)}}{2(c_1 c_2 - c_1 - c_2 + 1)}.$
4	<p>Compute the plug-in estimator of the limiting mean of the squared alignment:</p> $\hat{\mu}_i = \frac{1}{1 + d(\hat{r}_i)}.$

3.2 Estimation of the Asymptotic Variance

The limiting mean alone does not fully describe the behavior of the squared alignment. Theorem 2.5 further shows that

$$\sqrt{n} \left(\langle \mathbf{u}_i, \boldsymbol{\nu}_i \rangle^2 - \frac{1}{1 + d(r_i)} \right) \xrightarrow{D} \mathcal{N}(0, \sigma^2(r_i) / (1 + d(r_i))^4).$$

Thus the corresponding asymptotic variance is

$$\tau_i^2 := \frac{\sigma^2(r_i)}{(1 + d(r_i))^4}.$$

This quantity measures the fluctuation scale of the squared alignment around its limiting mean. As in the previous subsection, we estimate τ_i^2 by substituting \hat{r}_i into the deterministic expression above.

Proposition 3.3. *Under the assumptions of Proposition 3.1, further assume that $\sigma^2(\cdot)$ is*

continuous at r_i , and that $0 < \sigma^2(r_i) < \infty$. Define

$$\hat{\tau}_i^2 := \frac{\sigma^2(\hat{r}_i)}{(1 + d(\hat{r}_i))^4}, \quad \hat{\tau}_i := \sqrt{\hat{\tau}_i^2},$$

on the event where $\hat{\tau}_i^2 \geq 0$. Then

$$\hat{\tau}_i^2 \xrightarrow{p} \tau_i^2, \quad \hat{\tau}_i \xrightarrow{p} \tau_i.$$

The proof is postponed to Section 8.

Remark 3.4. Proposition 3.3 shows that the asymptotic variance appearing in Theorem 2.5 is likewise estimable from the sample. Consequently, one can estimate not only the limiting mean of the squared alignment itself, but also the scale of its random fluctuation. In this sense, Propositions 3.1 and 3.3 provide complementary information: $\hat{\mu}_i$ estimates the limiting mean of the squared alignment, whereas $\hat{\tau}_i$ estimates its fluctuation scale.

3.3 A Real-Data Illustration

Since the population canonical directions are unobservable in real data, the quantity

$$\langle \mathbf{u}_i, \boldsymbol{\nu}_i \rangle^2$$

cannot be evaluated directly. Accordingly, the purpose of this subsection is not to validate the population-level limit in Theorem 2.4, but rather to illustrate how the plug-in estimator proposed in Proposition 3.1 can be used to assess the quality of the leading sample canonical directions in practice. The real-data illustration focuses on the first-order estimator $\hat{\mu}_i$, since the main purpose is to assess the recovery quality of the detected sample direction.

We consider the limestone grassland community data originally reported in Table A-2 of Gittins [12]. The data contain $n = 45$ sampling sites from a limestone grassland community in Anglesey, North Wales, and include two blocks of variables: an 8-dimensional block of plant species abundances and a 6-dimensional block of soil characteristics. The same dataset was also used in Bao et al. [8] as a real-data example for high-dimensional canonical correlation analysis. Following the standard CCA preprocessing used there, we first center all variables across samples and then form the sample canonical correlation matrix from the centered data.

Let \mathbf{X} and \mathbf{Y} denote the centered species and soil data matrices, with dimensions $p \times n$ and $q \times n$, respectively. We then form the sample canonical correlation matrix

$$\mathbf{S}_{xx}^{-1} \mathbf{S}_{xy} \mathbf{S}_{yy}^{-1} \mathbf{S}_{yx},$$

and compute its leading eigenvalues l_i . The six sample squared canonical correlations computed from the centered Table A-2 data of Gittins [12] are

$$l_1 = 0.8293, \quad l_2 = 0.5198, \quad l_3 = 0.3589, \quad l_4 = 0.1074, \quad l_5 = 0.0938, \quad l_6 = 0.0378.$$

Here $p = 8, q = 6$, and $n = 45$, and the corresponding upper edge is $d_+ = 0.5236$. Thus only the first sample eigenvalue satisfies $l_1 > d_+$. The remaining eigenvalues all lie below the threshold, with the second eigenvalue $l_2 = 0.5198$ being close to, but still below, d_+ . This

suggests that the data contain one statistically separated leading direction. In other words, the dominant association between the species block and the soil block is essentially captured by a single leading canonical direction.

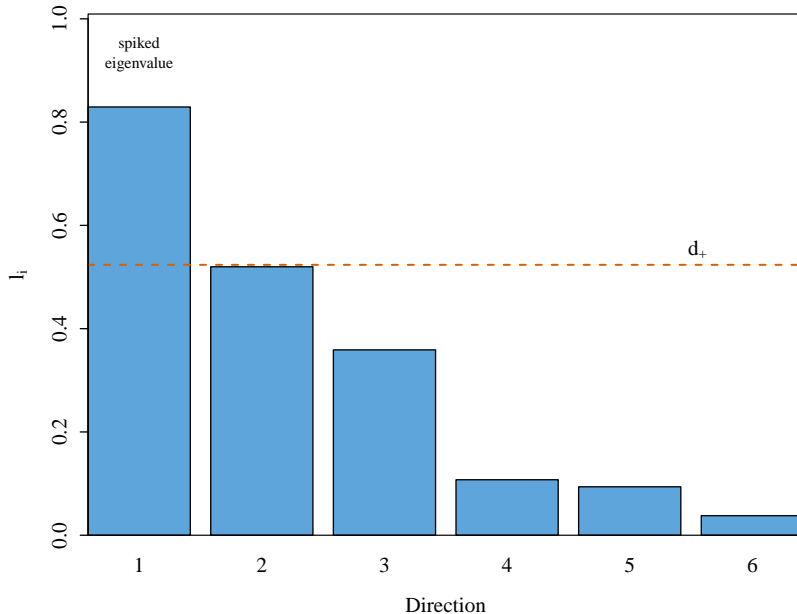


Figure 1: Sample squared canonical correlations for the limestone grassland community data. The dashed horizontal line indicates the upper edge $d_+ = 0.5236$. Only the first eigenvalue is identified as a sample spiked eigenvalue.

We next apply the plug-in estimation procedure stated in Proposition 3.1 to this separated direction. For the sample spiked eigenvalue $l_1 = 0.8293$, we define

$$\hat{r}_1 := \gamma^{-1}(l_1), \quad \hat{\mu}_1 := \frac{1}{1 + d(\hat{r}_1)}.$$

This gives

$$\hat{r}_1 = 0.7494, \quad \hat{\mu}_1 = 0.8155.$$

The value of l_1 indicates that the first direction is detectable from the sample spectrum, whereas $\hat{\mu}_1$ gives a different type of information: it quantifies the estimated asymptotic alignment between the first sample canonical direction and its population counterpart. Thus, the first direction in this dataset is not only separated from the bulk, but is also estimated to have relatively high recovery quality.

Table 2: The leading sample canonical direction and its estimated recovery quality.

Quantity	Value
ν_1	(0.7670, 0.5141, 0.1644, 0.1037, -0.0952, 0.1547, 0.1197, -0.2495)
ξ_1	(0.2968, 0.4852, 0.7982, 0.0840, -0.1542, -0.0924)
l_1	0.8293
\hat{r}_1	0.7494
$\hat{\mu}_1$	0.8155

The vectors ν_1 and ξ_1 in Table 2 are the two sample canonical direction vectors associated with the first sample spiked eigenvalue l_1 , on the species and soil sides, respectively. They should not be interpreted as consistent estimates of the corresponding population directions. Rather, they identify which variables contribute most to the leading sample direction, while the plug-in estimator $\hat{\mu}_1$ provides the corresponding assessment of recovery quality. On the species side, the first sample canonical direction has its largest coefficients on the first two variables, whose coefficients are 0.7670 and 0.5141. On the soil side, the largest coefficient is attached to the third soil variable, with coefficient 0.7982, while the first two soil variables also have positive contributions. Under the sign convention used in the table, the fifth and sixth soil variables have negative coefficients. Thus, at the sample level, the leading canonical direction is primarily determined by a small number of variables from each block. The value $\hat{\mu}_1 = 0.8155$ further indicates that this empirically observed direction has relatively high estimated alignment with its population counterpart. Therefore, the loading vectors provide a sample-level interpretation of the leading direction, whereas $\hat{\mu}_1$ quantifies the reliability of this interpretation under the high-dimensional asymptotic framework.

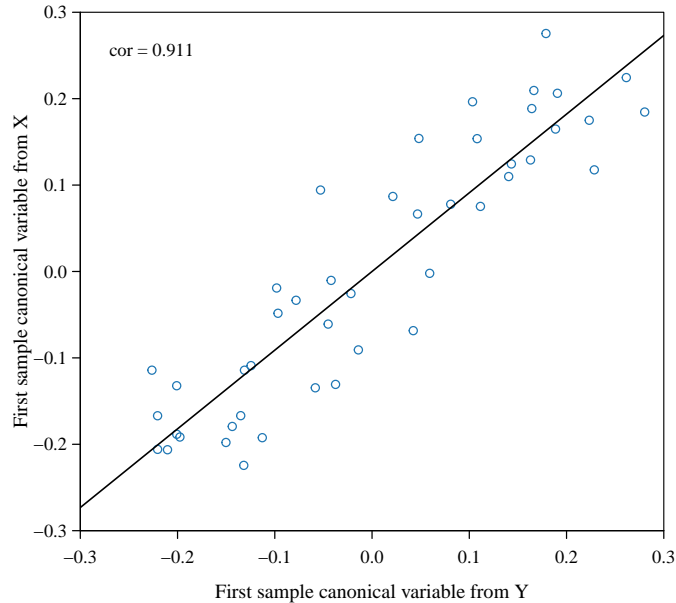


Figure 2: Scatter plot of the first pair of sample canonical variates for the limestone grassland community data.

Figure 2 plots the first pair of sample variates $\nu_1^\top \mathbf{X}$ and $\xi_1^\top \mathbf{Y}$. The sample correlation between them is approximately

$$\sqrt{l_1} = 0.9107.$$

The points display a clear positive linear trend, which is consistent with the large first squared canonical correlation. This plot describes the sample-level association between the two canonical variates. The plug-in estimator $\hat{\mu}_1$, on the other hand, provides an estimate of the population-level recovery quality: it measures how reliably the corresponding sample direction represents its population counterpart under the high-dimensional asymptotic framework.

This example illustrates the additional information provided by the proposed plug-in esti-

mator. The inequality $l_1 > d_+$ shows that the leading direction is detectable from the sample spectrum, but it does not by itself indicate whether the corresponding sample direction is a reliable representative of the population direction. The estimator $\hat{\mu}_1$ addresses this second question. In the present dataset, $\hat{\mu}_1 = 0.8155$ suggests that the leading sample canonical direction retains a substantial amount of population-level directional information. Thus, the proposed estimator does not merely restate the presence of a sample spiked eigenvalue; rather, it quantifies the recovery quality of the associated sample direction.

This distinction is important in the high-dimensional regime. Since sample canonical directions are generally not consistent estimators of their population counterparts, the direct recovery of the population directions is no longer the appropriate benchmark. A more relevant question is how much population-level structural information is preserved by the sample directions. Theorem 2.4 provides a quantitative answer to this question through the limit of the squared alignment, and Proposition 3.1 makes this quantity estimable from the data. In this sense, $\hat{\mu}_i$ turns the non-consistency of sample canonical directions into a data-based measure of recovery quality, thereby complementing the usual eigenvalue-based detection of spiked directions.

4 Simulation

We conduct Monte Carlo simulations to examine the finite-sample performance of the first-order limit and the Gaussian fluctuation stated in Theorems 2.4 and 2.5. Throughout, we take $p = \lfloor c_1 n \rfloor$ and $q = \lfloor c_2 n \rfloor$ with $(c_1, c_2) = (0.5, 0.3)$. The data matrices are generated under the Gaussian model: the entries $\{y_{ij}\}$ and $\{w_{ij}\}$ are independent and identically distributed (i.i.d.) as $\mathcal{N}(0, 1/n)$. The simulations have two goals: to illustrate the convergence of $\langle \mathbf{u}_i, \boldsymbol{\nu}_i \rangle^2$ to its deterministic limit, and to assess the normal approximation after the standardization in Theorem 2.5. For each value of n , we repeat the experiment independently 5000 times and compute $\langle \mathbf{u}_i, \boldsymbol{\nu}_i \rangle^2$ in each repetition.

We consider two population canonical correlation structures. In the first setting, the population spike structure has rank one, with a single spike $r_1 = 0.8$. In the second setting, $\boldsymbol{\Lambda} \boldsymbol{\Lambda}^\top$ has rank three, with spikes $r_1 = 0.86$, $r_2 = 0.81$, and $r_3 = 0.76$. For $(c_1, c_2) = (0.5, 0.3)$, the phase-transition threshold is

$$r_c = \sqrt{\frac{c_1 c_2}{(1 - c_1)(1 - c_2)}} \approx 0.655.$$

In both settings, the spikes are chosen above the phase-transition threshold, so that the associated sample eigenvalues separate from the bulk.

We first examine the deterministic limit in Theorem 2.4. For the rank-one setting, Figure 3 displays, for $n \in \{400, 800, 1200, 1600, 2000, 2400, 2800, 3200, 3600, 4000\}$, the boxplots of $\langle \mathbf{u}_1, \boldsymbol{\nu}_1 \rangle^2$ over 5000 repetitions, together with the corresponding Monte Carlo mean curve. As n increases, the empirical distribution becomes more concentrated; both the interquartile range and the whiskers shrink. The Monte Carlo mean approaches the deterministic limit $1/(1+d(r_1))$ predicted by Theorem 2.4. A mild finite-sample deviation from the theoretical limit is observed at small n (e.g., $n = 400$), but it diminishes rapidly as n grows, indicating a stable convergence to the theoretical limit.

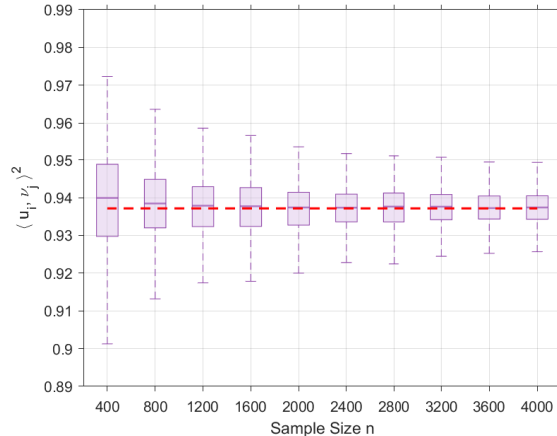


Figure 3: Rank-one setting: boxplots of $\langle \mathbf{u}_1, \boldsymbol{\nu}_1 \rangle^2$ over 5000 repetitions for $n \in \{400, 800, \dots, 4000\}$, illustrating the first-order limit in Theorem 2.4.

We next investigate the fluctuation result in Theorem 2.5. Still in the rank-one setting, we fix a large sample size $n = 4000$ and standardize $\langle \mathbf{u}_1, \boldsymbol{\nu}_1 \rangle^2$ according to Theorem 2.5:

$$Z_1 = \frac{\sqrt{n} \left(\langle \mathbf{u}_1, \boldsymbol{\nu}_1 \rangle^2 - 1/(1 + d(r_1)) \right)}{\sigma(r_1)/(1 + d(r_1))^2}.$$

Here and below, $\sigma(r_i) = \sqrt{\sigma^2(r_i)}$. Figure 4 shows the histogram of Z_1 based on 5000 repetitions, overlaid with the $\mathcal{N}(0, 1)$ density. The empirical histogram agrees well with the standard normal density, supporting the Gaussian approximation in Theorem 2.5 for large but finite n .

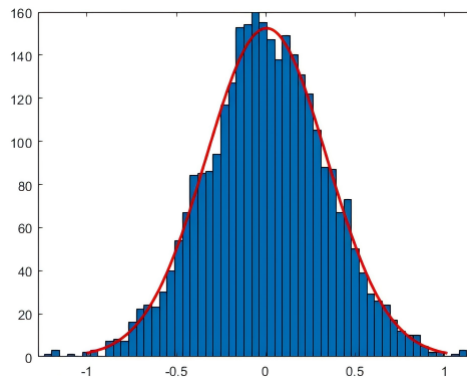


Figure 4: Rank-one setting: histogram of the standardized statistic Z_1 at $n = 4000$ over 5000 repetitions, overlaid with the $\mathcal{N}(0, 1)$ density, supporting the Gaussian approximation in Theorem 2.5.

We then turn to the rank-three setting. For each spike r_i ($i = 1, 2, 3$), we compute $\langle \mathbf{u}_i, \boldsymbol{\nu}_i \rangle^2$ over repeated Monte Carlo simulations and plot the running empirical mean against the number of repetitions. Figure 5 displays the convergence trajectories together with the corresponding theoretical first-order limits. The three panels show that the running averages stabilize around their predicted limits, providing numerical support for the first-order asymptotic theory. The convergence behavior varies across the three spike components. In all three cases, the running empirical means fluctuate around their corresponding theoretical first-order limits and gradually

stabilize as the number of repetitions increases. The components associated with stronger spikes, such as r_1 and r_2 , settle near their limiting values after the initial transient fluctuations. The weakest spike r_3 displays a more pronounced initial deviation and a slower stabilization pattern. Overall, these numerical results are broadly consistent with the theoretical prediction that stronger spectral separation improves the stability of the associated squared alignment.

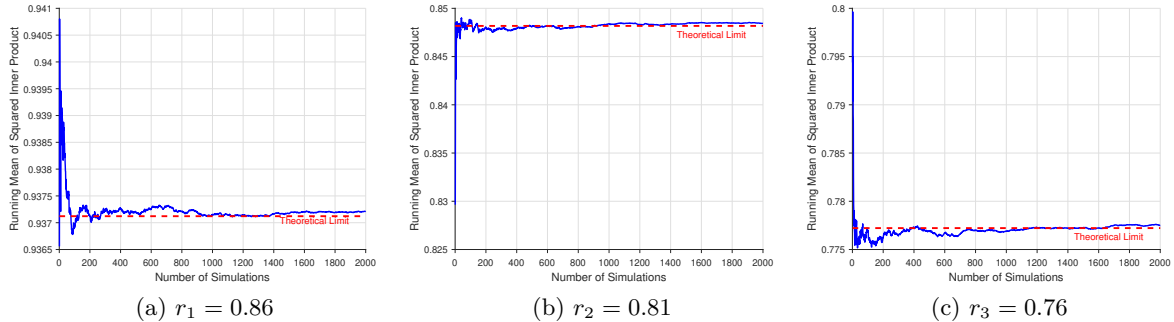


Figure 5: Rank-three setting: convergence trajectories of the running means of $\langle \mathbf{u}_i, \mathbf{v}_i \rangle^2$ ($i = 1, 2, 3$) over 5000 repetitions, illustrating the first-order limits and the dependence on signal strength.

Finally, we assess the Gaussian fluctuation in the rank-three setting. For $n \in \{2000, 4000, 6000\}$, we form the standardized statistics

$$Z_i = \frac{\sqrt{n} \left(\langle \mathbf{u}_i, \mathbf{v}_i \rangle^2 - 1/(1 + d(r_i)) \right)}{\sigma(r_i)/(1 + d(r_i))^2}, \quad i = 1, 2, 3,$$

and repeat the experiment 5000 times. Figures 6–8 provide three complementary diagnostics for the asymptotic normality of the standardized statistics Z_i ($i = 1, 2, 3$) in the rank-three setting. Figure 6 shows the empirical histograms at $n = 2000$, overlaid with the standard normal density. The histograms are centered near zero and exhibit an approximately bell-shaped profile, indicating that the normal approximation is already visible at this sample size. Figure 7 presents the corresponding Q-Q plots at $n = 4000$. The sample quantiles lie close to the reference normal line for all three spiked components, which confirms the normal approximation from a quantile perspective. Mild deviations appear mainly in the tails, as is typical in finite-sample simulations. Figure 8 compares the empirical distribution functions at $n = 6000$ with the standard normal distribution function. The empirical CDFs almost overlap with the theoretical CDF, showing good agreement at the level of the full distribution function. Overall, these graphical diagnostics demonstrate that the finite-sample behavior of the standardized statistics Z_i is consistent with the asymptotic normality result established in Theorem 2.5.

5 Proof of Main Theorems

This section outlines the main proof strategy. We first use the characteristic equation to transform the eigenvector projection problem into a problem concerning quadratic forms of resolvent matrices. We then demonstrate how the proofs of our main results, Theorem 2.4 and 2.5, are reduced to the computation of the deterministic limits and fluctuations of these quadratic forms,

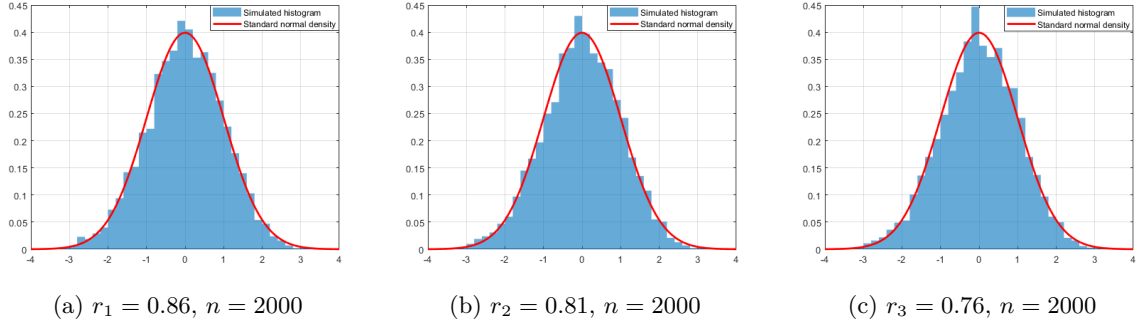


Figure 6: Rank-three setting: histograms of the standardized statistics Z_i ($i = 1, 2, 3$) at $n = 2000$ over 5000 repetitions, overlaid with the $\mathcal{N}(0, 1)$ density.

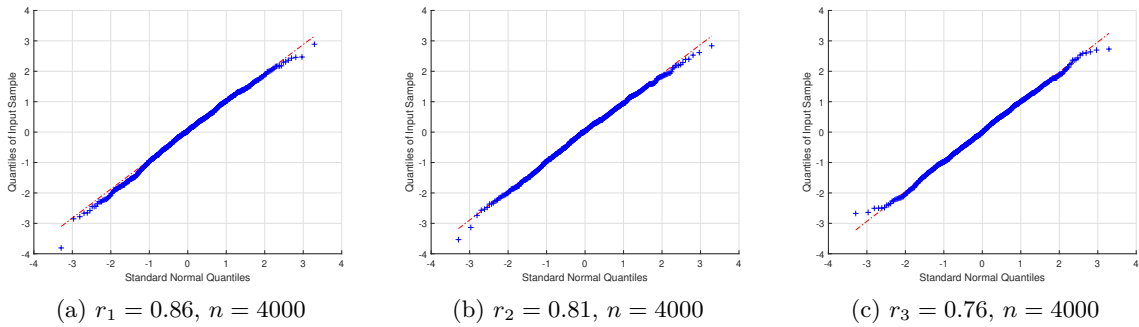


Figure 7: Rank-three setting: Q-Q plots of the standardized statistics Z_i ($i = 1, 2, 3$) at $n = 4000$ against the standard normal distribution.

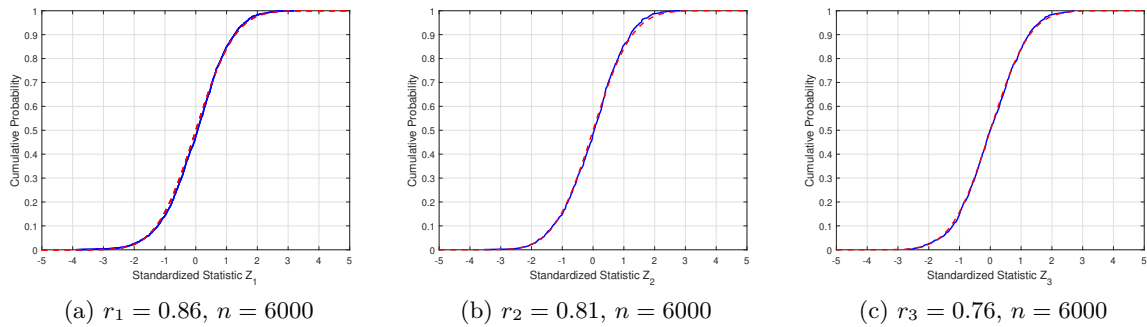


Figure 8: Rank-three setting: empirical distribution functions of the standardized statistics Z_i ($i = 1, 2, 3$) at $n = 6000$, compared with the standard normal distribution function.

which are established in the subsequent technical lemmas.

5.1 Schur Complement Reduction

Consider the following characteristic equation:

$$\mathbf{S}_{xy}\mathbf{S}_{yy}^{-1}\mathbf{S}_{yx}\boldsymbol{\nu}_i = l_i\mathbf{S}_{xx}\boldsymbol{\nu}_i,$$

i.e.,

$$(\mathbf{S}_{xy}\mathbf{S}_{yy}^{-1}\mathbf{S}_{yx} - l_i\mathbf{S}_{xx})\boldsymbol{\nu}_i = 0,$$

where l_i is the i -th eigenvalue of $\mathbf{S}_{xx}^{-1}\mathbf{S}_{xy}\mathbf{S}_{yy}^{-1}\mathbf{S}_{yx}$, and $\boldsymbol{\nu}_i$ is the eigenvector corresponding to the eigenvalue l_i . Using the model $\mathbf{X} = \boldsymbol{\Lambda}\mathbf{Y} + \boldsymbol{\Gamma}\mathbf{W}$ and the definitions of the sample covariance matrices, we can write $\mathbf{S}_{xx} = \mathbf{X}\mathbf{X}^\top$ and $\mathbf{S}_{xy}\mathbf{S}_{yy}^{-1}\mathbf{S}_{yx} = \mathbf{X}\mathbf{P}_y\mathbf{X}^\top$, where $\mathbf{P}_y = \mathbf{Y}^\top(\mathbf{Y}\mathbf{Y}^\top)^{-1}\mathbf{Y}$. Note that \mathbf{P}_y is an orthogonal projector: $\mathbf{P}_y^\top = \mathbf{P}_y$ and $\mathbf{P}_y^2 = \mathbf{P}_y$. The equation becomes $(\mathbf{X}\mathbf{P}_y\mathbf{X}^\top - l_i\mathbf{X}\mathbf{X}^\top)\boldsymbol{\nu}_i = 0$, or

$$\mathbf{X}(\mathbf{P}_y - l_i\mathbf{I}_n)\mathbf{X}^\top\boldsymbol{\nu}_i = 0.$$

Let $\boldsymbol{\Lambda}$ have the SVD $\boldsymbol{\Lambda} = \mathbf{U} \begin{pmatrix} \boldsymbol{\Lambda}_k & \mathbf{0} \\ \mathbf{0} & \mathbf{0} \end{pmatrix} \mathbf{V}^\top$, where $\mathbf{U} = (\mathbf{U}_1, \mathbf{U}_2) \in \mathbb{R}^{p \times p}$, $\mathbf{V} = (\mathbf{V}_1, \mathbf{V}_2) \in \mathbb{R}^{q \times q}$ are orthogonal, and $\boldsymbol{\Lambda}_k \in \mathbb{R}^{k \times k}$ satisfies $\boldsymbol{\Lambda}_k\boldsymbol{\Lambda}_k^\top = \text{diag}(r_1, \dots, r_k)$. We also write $\boldsymbol{\Gamma} = \mathbf{U}\text{diag}(\boldsymbol{\Gamma}_k, \mathbf{I}_{p-k})\mathbf{U}^\top$ with $\boldsymbol{\Gamma}_k = \text{diag}(\sqrt{1-r_1}, \dots, \sqrt{1-r_k})$. We further analyze the block matrix form of the characteristic equation. Let $\mathbf{U} = (\mathbf{U}_1, \mathbf{U}_2)$ where \mathbf{U}_1 consists of the first k columns (the population spiked eigenvectors) and \mathbf{U}_2 the remaining $p-k$. Substituting the model for \mathbf{X} , we have that $\boldsymbol{\nu}_i$ satisfies

$$\begin{aligned} (\mathbf{U}_1, \mathbf{U}_2) & \left(\begin{pmatrix} \boldsymbol{\Lambda}_k & \mathbf{0} \\ \mathbf{0} & \mathbf{0} \end{pmatrix} (\mathbf{V}_1, \mathbf{V}_2)^\top \mathbf{Y} + \begin{pmatrix} \boldsymbol{\Gamma}_k & \mathbf{0} \\ \mathbf{0} & \mathbf{I}_{p-k} \end{pmatrix} \mathbf{U}^\top \mathbf{W} \right) (\mathbf{P}_y - l_i\mathbf{I}_n) \\ & \times \left(\mathbf{Y}^\top (\mathbf{V}_1, \mathbf{V}_2) \begin{pmatrix} \boldsymbol{\Lambda}_k & \mathbf{0} \\ \mathbf{0} & \mathbf{0} \end{pmatrix} + \mathbf{W}^\top \mathbf{U} \begin{pmatrix} \boldsymbol{\Gamma}_k & \mathbf{0} \\ \mathbf{0} & \mathbf{I}_{p-k} \end{pmatrix} \right) \begin{pmatrix} \mathbf{U}_1^\top \\ \mathbf{U}_2^\top \end{pmatrix} \boldsymbol{\nu}_i = 0, \end{aligned}$$

expanding this yields:

$$(\mathbf{U}_1, \mathbf{U}_2) \begin{pmatrix} \mathbf{A} & \mathbf{B} \\ \mathbf{C} & \mathbf{D} \end{pmatrix} \begin{pmatrix} \boldsymbol{\varpi}_{i1} \\ \boldsymbol{\varpi}_{i2} \end{pmatrix} = 0,$$

where $\boldsymbol{\varpi}_{i1} = \mathbf{U}_1^\top \boldsymbol{\nu}_i$ (a $k \times 1$ vector) and $\boldsymbol{\varpi}_{i2} = \mathbf{U}_2^\top \boldsymbol{\nu}_i$ (a $(p-k) \times 1$ vector). The matrices are defined as

$$\begin{aligned} \mathbf{A} &= \mathbf{A}(l_i) := (\boldsymbol{\Lambda}_k \mathbf{V}_1^\top \mathbf{Y} + \boldsymbol{\Gamma}_k \mathbf{U}_1^\top \mathbf{W})(\mathbf{P}_y - l_i\mathbf{I}_n)(\mathbf{Y}^\top \mathbf{V}_1 \boldsymbol{\Lambda}_k + \mathbf{W}^\top \mathbf{U}_1 \boldsymbol{\Gamma}_k), \\ \mathbf{B} &= \mathbf{B}(l_i) := (\boldsymbol{\Lambda}_k \mathbf{V}_1^\top \mathbf{Y} + \boldsymbol{\Gamma}_k \mathbf{U}_1^\top \mathbf{W})(\mathbf{P}_y - l_i\mathbf{I}_n)\mathbf{W}^\top \mathbf{U}_2, \\ \mathbf{C} &= \mathbf{C}(l_i) := \mathbf{U}_2^\top \mathbf{W}(\mathbf{P}_y - l_i\mathbf{I}_n)(\mathbf{Y}^\top \mathbf{V}_1 \boldsymbol{\Lambda}_k + \mathbf{W}^\top \mathbf{U}_1 \boldsymbol{\Gamma}_k), \\ \mathbf{D} &= \mathbf{D}(l_i) := \mathbf{U}_2^\top \mathbf{W}(\mathbf{P}_y - l_i\mathbf{I}_n)\mathbf{W}^\top \mathbf{U}_2. \end{aligned}$$

Since l_i is a sample spike and $l_i \xrightarrow{a.s.} \gamma_i$, on an event whose probability tends to one, the matrix $\mathbf{D}(l_i) = \mathbf{U}_2^\top \mathbf{W}(\mathbf{P}_y - l_i \mathbf{I}_n) \mathbf{W}^\top \mathbf{U}_2$ is invertible. On this event, we may apply the Schur complement to the block matrix above.

$$(\mathbf{U}_1, \mathbf{U}_2) \begin{pmatrix} \mathbf{I}_k & \mathbf{B}\mathbf{D}^{-1} \\ 0 & \mathbf{I}_{p-k} \end{pmatrix} \begin{pmatrix} \mathbf{A} - \mathbf{B}\mathbf{D}^{-1}\mathbf{C} & \mathbf{0} \\ \mathbf{0} & \mathbf{D} \end{pmatrix} \begin{pmatrix} \boldsymbol{\varpi}_{i1} \\ \mathbf{D}^{-1}\mathbf{C}\boldsymbol{\varpi}_{i1} + \boldsymbol{\varpi}_{i2} \end{pmatrix} = 0,$$

This yields the equivalent system of equations:

$$\begin{cases} (\mathbf{A} - \mathbf{B}\mathbf{D}^{-1}\mathbf{C})\boldsymbol{\varpi}_{i1} = 0, \\ \mathbf{C}\boldsymbol{\varpi}_{i1} + \mathbf{D}\boldsymbol{\varpi}_{i2} = 0, \end{cases}$$

which implies

$$\begin{cases} (\mathbf{A} - \mathbf{B}\mathbf{D}^{-1}\mathbf{C})\boldsymbol{\varpi}_{i1} = 0, \\ \boldsymbol{\varpi}_{i2} = -\mathbf{D}^{-1}\mathbf{C}\boldsymbol{\varpi}_{i1}. \end{cases} \quad (9)$$

The first equation determines the direction of $\boldsymbol{\varpi}_{i1}$, while the second equation links $\boldsymbol{\varpi}_{i2}$ to $\boldsymbol{\varpi}_{i1}$. The vector of interest is $\boldsymbol{\varpi}_{i1}$, which contains the projections $\langle \mathbf{u}_j, \boldsymbol{\nu}_i \rangle$ for $j = 1, \dots, k$. Since $\boldsymbol{\nu}_i$ has unit norm, we have $\|\boldsymbol{\varpi}_{i1}\|^2 + \|\boldsymbol{\varpi}_{i2}\|^2 = 1$. Substituting the second equation of (9) gives the normalization constraint:

$$\boldsymbol{\varpi}_{i1}^\top \boldsymbol{\varpi}_{i1} + \boldsymbol{\varpi}_{i1}^\top \mathbf{C}^\top (\mathbf{D}^{-1})^\top \mathbf{D}^{-1} \mathbf{C} \boldsymbol{\varpi}_{i1} = 1.$$

Since \mathbf{D} is symmetric, this simplifies to

$$\boldsymbol{\varpi}_{i1}^\top \left(\mathbf{I}_k + \mathbf{C}^\top \mathbf{D}^{-2} \mathbf{C} \right) \boldsymbol{\varpi}_{i1} = 1. \quad (10)$$

The k -dimensional matrix $\mathbf{A} - \mathbf{B}\mathbf{D}^{-1}\mathbf{C}$ above is consistent with the content shown in equation (4.13) of Bao et al. (2019) [8]. Let

$$M_\Lambda(z) := \mathbf{A}(z) - \mathbf{B}(z)\mathbf{D}(z)^{-1}\mathbf{C}(z)$$

be the (random) $k \times k$ matrix-valued function arising from the Schur complement. For the i -th sample outlier l_i with limit γ_i , we invoke (6.9) of [8]. In particular, for $\alpha, \beta \in I_i$ (the index set associated with the population spike r_i), there exists a random matrix \mathcal{R} (defined in Lemma 6.2 of [8]) such that

$$(M_\Lambda)_{\alpha\beta}(l_i) = M_{\alpha\beta}(\gamma_i) - \delta_{\alpha\beta} \Delta_{ii} (l_i - \gamma_i) (1 + o_p(1)) + \frac{1}{\sqrt{n}} \mathcal{R}_{\alpha\beta} + o_p(n^{-1/2}), \quad (11)$$

where $M(z)$ is a deterministic diagonal matrix with diagonal entries $m_j(z)$ and Δ is also diagonal. Moreover, $m_j(\gamma_j) = 0$ for each j . Let \mathcal{J}_i denote the index set of population eigenvalues equal to r_i . For the simple spike r_i , we have

$$(M_\Lambda)_{ii}(l_i) = O_p(n^{-1/2}).$$

Moreover, the off-diagonal blocks satisfy

$$(M_\Lambda(l_i))_{-i,i} = O_p(n^{-1/2}), \quad (M_\Lambda(l_i))_{i,-i} = O_p(n^{-1/2}).$$

For $j \neq i$, since $m_j(\gamma_i) \neq 0$, the diagonal entries of $M(\gamma_i)$ in the $(-i, -i)$ block are bounded away from zero. Hence

$$(M_\Lambda(l_i))_{-i,-i} = (M(\gamma_i))_{-i,-i} + O_p(n^{-1/2})$$

is invertible with probability tending to one, and

$$\|(M_\Lambda(l_i))_{-i,-i}^{-1}\| = O_p(1).$$

Therefore, from the equation $M_\Lambda(l_i)\boldsymbol{\varpi}_{i1} = 0$ we obtain

$$\boldsymbol{\varpi}_{i1,-i} = -(M_\Lambda(l_i))_{-i,-i}^{-1}(M_\Lambda(l_i))_{-i,i} \boldsymbol{\varpi}_{i1,i} = O_p(n^{-1/2}) \boldsymbol{\varpi}_{i1,i},$$

which shows that all components of $\boldsymbol{\varpi}_{i1}$ except the i -th one are of order $O_p(n^{-1/2})$. Thus, under the simple spike assumption $\mathcal{J}_i = \{i\}$,

$$\boldsymbol{\varpi}_{i1,-i} = O_p(n^{-1/2}) \boldsymbol{\varpi}_{i1,i}.$$

Since $\|\boldsymbol{\nu}_i\| = 1$, we have $\boldsymbol{\varpi}_{i1,i} = O_p(1)$, and hence

$$\|\boldsymbol{\varpi}_{i1,-i}\| = O_p(n^{-1/2}).$$

Let

$$\mathbf{M}_i := \mathbf{I}_k + \mathbf{C}^\top \mathbf{D}^{-2} \mathbf{C}.$$

From the Schur complement reduction, we have

$$\boldsymbol{\varpi}_{i1}^\top \mathbf{M}_i \boldsymbol{\varpi}_{i1} = 1.$$

Moreover, for a simple spike r_i ,

$$\boldsymbol{\varpi}_{i1,-i} = O_p(n^{-1/2}) \boldsymbol{\varpi}_{i1,i}.$$

Since $\|\boldsymbol{\nu}_i\| = 1$, we have $\boldsymbol{\varpi}_{i1,i} = O_p(1)$, and hence

$$\|\boldsymbol{\varpi}_{i1,-i}\| = O_p(n^{-1/2}).$$

Define

$$\mathbf{r}_i = \boldsymbol{\varpi}_{i1} - \boldsymbol{\varpi}_{i1,i} \mathbf{e}_i.$$

Then the i -th component of \mathbf{r}_i is zero and

$$\boldsymbol{\varpi}_{i1} = \boldsymbol{\varpi}_{i1,i} \mathbf{e}_i + \mathbf{r}_i, \quad \|\mathbf{r}_i\| = O_p(n^{-1/2}).$$

Substituting this decomposition into the normalization constraint gives

$$1 = \varpi_{i1,i}^2 [\mathbf{M}_i]_{ii} + 2\varpi_{i1,i} \mathbf{e}_i^\top \mathbf{M}_i \mathbf{r}_i + \mathbf{r}_i^\top \mathbf{M}_i \mathbf{r}_i.$$

By Lemma 5.1, for $j \neq i$,

$$[\mathbf{M}_i]_{ij} = O_p(n^{-1/2}).$$

Since the i -th component of \mathbf{r}_i is zero and k is fixed,

$$\mathbf{e}_i^\top \mathbf{M}_i \mathbf{r}_i = \sum_{j \neq i} [\mathbf{M}_i]_{ij} (\mathbf{r}_i)_j = O_p(n^{-1}).$$

Also, since $\|\mathbf{M}_i\| = O_p(1)$,

$$\mathbf{r}_i^\top \mathbf{M}_i \mathbf{r}_i = O_p(n^{-1}).$$

Therefore,

$$1 = \varpi_{i1,i}^2 [\mathbf{M}_i]_{ii} + O_p(n^{-1}).$$

Recalling that

$$\varpi_{i1,i}^2 = \langle \mathbf{u}_i, \boldsymbol{\nu}_i \rangle^2,$$

we obtain the strengthened normalization reduction

$$\langle \mathbf{u}_i, \boldsymbol{\nu}_i \rangle^2 [\mathbf{M}_i]_{ii} = 1 + O_p(n^{-1}).$$

This strengthened reduction is sufficient for both the first-order limit and the second-order fluctuation. Therefore, up to the order needed for the first- and second-order analysis, the behavior of $\langle \mathbf{u}_i, \boldsymbol{\nu}_i \rangle^2$ is governed by the i -th diagonal entry of \mathbf{M}_i . Recalling the definitions of matrices \mathbf{C} and \mathbf{D} , we obtain the decomposition:

$$\begin{aligned} & \mathbf{M}_i \\ = & \mathbf{I}_k \\ & + \boldsymbol{\Gamma}_k \mathbf{U}_1^\top \mathbf{W} (\mathbf{P}_y - l_i \mathbf{I}_n) \mathbf{W}^\top \mathbf{U}_2 \left(\mathbf{U}_2^\top \mathbf{W} (\mathbf{P}_y - l_i \mathbf{I}_n) \mathbf{W}^\top \mathbf{U}_2 \right)^{-2} \mathbf{U}_2^\top \mathbf{W} (\mathbf{P}_y - l_i \mathbf{I}_n) \mathbf{W}^\top \mathbf{U}_1 \boldsymbol{\Gamma}_k \\ & + \boldsymbol{\Lambda}_k \mathbf{V}_1^\top \mathbf{Y} (\mathbf{P}_y - l_i \mathbf{I}_n) \mathbf{W}^\top \mathbf{U}_2 \left(\mathbf{U}_2^\top \mathbf{W} (\mathbf{P}_y - l_i \mathbf{I}_n) \mathbf{W}^\top \mathbf{U}_2 \right)^{-2} \mathbf{U}_2^\top \mathbf{W} (\mathbf{P}_y - l_i \mathbf{I}_n) \mathbf{Y}^\top \mathbf{V}_1 \boldsymbol{\Lambda}_k \\ & + \boldsymbol{\Lambda}_k \mathbf{V}_1^\top \mathbf{Y} (\mathbf{P}_y - l_i \mathbf{I}_n) \mathbf{W}^\top \mathbf{U}_2 \left(\mathbf{U}_2^\top \mathbf{W} (\mathbf{P}_y - l_i \mathbf{I}_n) \mathbf{W}^\top \mathbf{U}_2 \right)^{-2} \mathbf{U}_2^\top \mathbf{W} (\mathbf{P}_y - l_i \mathbf{I}_n) \mathbf{W}^\top \mathbf{U}_1 \boldsymbol{\Gamma}_k \\ & + \boldsymbol{\Gamma}_k \mathbf{U}_1^\top \mathbf{W} (\mathbf{P}_y - l_i \mathbf{I}_n) \mathbf{W}^\top \mathbf{U}_2 \left(\mathbf{U}_2^\top \mathbf{W} (\mathbf{P}_y - l_i \mathbf{I}_n) \mathbf{W}^\top \mathbf{U}_2 \right)^{-2} \mathbf{U}_2^\top \mathbf{W} (\mathbf{P}_y - l_i \mathbf{I}_n) \mathbf{Y}^\top \mathbf{V}_1 \boldsymbol{\Lambda}_k \\ := & \mathbf{I}_k + I_{k1} + I_{k2} + I_{k3} + I_{k4}. \end{aligned} \tag{12}$$

Here \mathbf{D}^{-2} means $\mathbf{D}^{-1} \mathbf{D}^{-1}$. Our proofs now hinge on finding the limits and fluctuations of the diagonal elements of these four matrices.

5.2 Technical Lemmas

The Schur complement reduction above shows that the proofs of Theorems 2.4 and 2.5 depend on the asymptotic behavior of the entries of

$$\mathbf{M}_i := \mathbf{I}_k + \mathbf{C}^\top \mathbf{D}^{-2} \mathbf{C}.$$

Using the decomposition

$$\mathbf{M}_i = \mathbf{I}_k + I_{k1} + I_{k2} + I_{k3} + I_{k4},$$

we summarize the required deterministic limits, off-diagonal bounds, and fluctuation limits in the following two lemmas. Their proofs are given in Sections 6 and 7.

Lemma 5.1 (First-order expansion and off-diagonal control). *Under the assumptions of Theorem 2.4, fix a simple spike r_i . Then the i -th diagonal entry of \mathbf{M}_i satisfies*

$$[\mathbf{M}_i]_{ii} = 1 + d(r_i) + O_p(n^{-1/2}),$$

where $d(r_i)$ is the deterministic function appearing in Theorem 2.4. Moreover,

$$[I_{k3}]_{ii} = O_p(n^{-1/2}), \quad [I_{k4}]_{ii} = O_p(n^{-1/2}).$$

For any $a \neq b$, the off-diagonal entries satisfy

$$[I_{kj}]_{ab} = O_p(n^{-1/2}), \quad j = 1, 2, 3, 4.$$

Consequently,

$$[\mathbf{M}_i]_{ab} = O_p(n^{-1/2}), \quad a \neq b.$$

In particular,

$$\|\mathbf{M}_i\| = O_p(1).$$

Let \mathcal{V}_{k1} and \mathcal{V}_{k2} denote the centered $O_p(n^{-1/2})$ fluctuation terms of $[I_{k1}]_{ii}$ and $[I_{k2}]_{ii}$, respectively. More precisely, define

$$[\mathcal{V}_{k1}]_{ii} := [I_{k1}]_{ii} - \mathbb{E}\left([I_{k1}]_{ii} \mid \mathbf{Y}, \mathbf{U}_2^\top \mathbf{W}\right), \quad [\mathcal{V}_{k2}]_{ii} := [I_{k2}]_{ii} - \mathbb{E}\left([I_{k2}]_{ii} \mid \mathbf{Y}, \mathbf{U}_2^\top \mathbf{W}\right),$$

so that $\mathbb{E}([\mathcal{V}_{k1}]_{ii} \mid \mathbf{Y}, \mathbf{U}_2^\top \mathbf{W}) = \mathbb{E}([\mathcal{V}_{k2}]_{ii} \mid \mathbf{Y}, \mathbf{U}_2^\top \mathbf{W}) = 0$. The following lemma characterizes the limiting variances and covariances of all fluctuation terms.

Lemma 5.2 (Fluctuation of the normalization factor). *Under the assumptions of Theorem 2.5, let*

$$G_{i,n} := \sqrt{n} ([\mathbf{M}_i]_{ii} - 1 - d(r_i)).$$

Then

$$G_{i,n} \xrightarrow{D} \mathcal{N}(0, \sigma^2(r_i)).$$

More precisely, let

$$X_{1n} := \sqrt{n}[\mathcal{V}_{k1}]_{ii}, \quad X_{2n} := \sqrt{n}[\mathcal{V}_{k2}]_{ii}, \quad X_{3n} := \sqrt{n}[I_{k3} + I_{k4}]_{ii}.$$

Then

$$(X_{1n}, X_{2n}, X_{3n})$$

converges jointly in distribution to a centered Gaussian vector. Moreover,

$$G_{i,n} = X_{1n} + X_{2n} + X_{3n} + o_p(1).$$

The limiting variances are

$$\text{Var}(X_{1n}) = A_1(r_i) + o(1),$$

where

$$\begin{aligned} A_1(r_i) = & 2(1 - r_i)^2 P_1(r_i) - 4 \frac{\eta r_i - \omega}{r_i} (1 - r_i)^3 (P_1(r_i) + F_3(r_i)) \\ & + \frac{2(\eta r_i - \omega)^2}{r_i^2} (1 - r_i)^4 (P_1(r_i) + 2F_3(r_i) + Q_3(r_i)), \end{aligned}$$

$$\text{Var}(X_{2n}) = A_2(r_i) + o(1),$$

where

$$A_2(r_i) = \frac{2(\eta r_i - \omega)^4 (1 - r_i)^4}{r_i^2} (J_{k1}(r_i) + J_{k2}(r_i) + J_{k3}(r_i) + J_{k4}(r_i) + J_{k5}(r_i)),$$

and

$$\text{Var}(X_{3n}) = A_3(r_i) + o(1),$$

where

$$A_3(r_i) = \frac{4(\eta r_i - \omega)^3 (1 - r_i)^4 Q_4(r_i)}{c_2 r_i^2} + \frac{4c_1 (\eta r_i - \omega)^2 (1 - r_i)^3 Q_7(r_i)}{c_2 r_i}.$$

The scaled cross-covariances satisfy

$$\text{Cov}(X_{1n}, X_{2n}) = o(1), \quad \text{Cov}(X_{1n}, X_{3n}) = o(1), \quad \text{Cov}(X_{2n}, X_{3n}) = o(1).$$

Therefore,

$$\sigma^2(r_i) = A_1(r_i) + A_2(r_i) + A_3(r_i).$$

The deterministic quantities

$$P_1(r_i), \quad F_3(r_i), \quad Q_3(r_i), \quad J_{k\ell}(r_i), \quad \ell = 1, \dots, 5, \quad Q_4(r_i), \quad Q_7(r_i)$$

are defined in Section 7.

5.3 Proofs of Main Results

We now prove the main theorems, assuming Lemmas 5.1 and 5.2 hold.

Proof of Theorem 2.4. By Lemma 5.1,

$$[\mathbf{M}_i]_{ii} = 1 + d(r_i) + O_p(n^{-1/2}).$$

Together with the strengthened normalization reduction,

$$\langle \mathbf{u}_i, \boldsymbol{\nu}_i \rangle^2 [\mathbf{M}_i]_{ii} = 1 + O_p(n^{-1}),$$

we have

$$\langle \mathbf{u}_i, \boldsymbol{\nu}_i \rangle^2 = \frac{1 + O_p(n^{-1})}{1 + d(r_i) + O_p(n^{-1/2})}.$$

Since $1 + d(r_i) > 0$, the continuous mapping theorem gives

$$\langle \mathbf{u}_i, \boldsymbol{\nu}_i \rangle^2 \xrightarrow{p} \frac{1}{1 + d(r_i)}.$$

This proves Theorem 2.4. □

Proof of Theorem 2.5. By Lemma 5.2, we have

$$[\mathbf{M}_i]_{ii} = 1 + d(r_i) + n^{-1/2}G_{i,n} + o_p(n^{-1/2}),$$

where

$$G_{i,n} \xrightarrow{D} \mathcal{N}(0, \sigma^2(r_i)).$$

Using the strengthened normalization reduction,

$$\langle \mathbf{u}_i, \boldsymbol{\nu}_i \rangle^2 [\mathbf{M}_i]_{ii} = 1 + O_p(n^{-1}),$$

we obtain

$$\langle \mathbf{u}_i, \boldsymbol{\nu}_i \rangle^2 = \frac{1 + O_p(n^{-1})}{1 + d(r_i) + n^{-1/2}G_{i,n} + o_p(n^{-1/2})}.$$

Since $1 + d(r_i) > 0$, a first-order Taylor expansion yields

$$\langle \mathbf{u}_i, \boldsymbol{\nu}_i \rangle^2 = \frac{1}{1 + d(r_i)} - \frac{n^{-1/2}G_{i,n}}{(1 + d(r_i))^2} + o_p(n^{-1/2}).$$

Therefore,

$$\sqrt{n} \left(\langle \mathbf{u}_i, \boldsymbol{\nu}_i \rangle^2 - \frac{1}{1 + d(r_i)} \right) = -\frac{G_{i,n}}{(1 + d(r_i))^2} + o_p(1).$$

Since

$$G_{i,n} \xrightarrow{D} \mathcal{N}(0, \sigma^2(r_i)),$$

Slutsky's theorem implies

$$\sqrt{n} \left(\langle \mathbf{u}_i, \boldsymbol{\nu}_i \rangle^2 - \frac{1}{1 + d(r_i)} \right) \xrightarrow{D} \mathcal{N} \left(0, \frac{\sigma^2(r_i)}{(1 + d(r_i))^4} \right).$$

This proves Theorem 2.5. □

6 Proofs of Technical Lemmas

This section provides the proofs for the key technical lemmas, 5.1 and 5.2.

Proof of Lemma 5.1. Based on the decomposition in Section 5, write

$$I_{k1} = \mathbf{\Gamma}_k \mathbf{U}_1^\top \mathbf{W} (\mathbf{P}_y - l_i \mathbf{I}_n) \mathbf{W}^\top \mathbf{U}_2 \Phi^2(l_i) \mathbf{U}_2^\top \mathbf{W} (\mathbf{P}_y - l_i \mathbf{I}_n) \mathbf{W}^\top \mathbf{U}_1 \mathbf{\Gamma}_k,$$

where

$$\Phi(z) = \left(\mathbf{U}_2^\top \mathbf{W} (\mathbf{P}_y - z \mathbf{I}_n) \mathbf{W}^\top \mathbf{U}_2 \right)^{-1}.$$

Conditional on \mathbf{Y} and $\mathbf{U}_2^\top \mathbf{W}$, the rows of $\mathbf{U}_1^\top \mathbf{W}$ are independent centered Gaussian vectors with covariance $n^{-1} \mathbf{I}_n$. Hence

$$\mathbb{E}(I_{k1} \mid \mathbf{Y}, \mathbf{U}_2^\top \mathbf{W}) = \frac{1}{n} \text{tr} \left[(\mathbf{P}_y - l_i \mathbf{I}_n) \mathbf{W}^\top \mathbf{U}_2 \Phi^2(l_i) \mathbf{U}_2^\top \mathbf{W} (\mathbf{P}_y - l_i \mathbf{I}_n) \right] \mathbf{\Gamma}_k \mathbf{\Gamma}_k^\top.$$

Define

$$\mathcal{V}_{k1} := I_{k1} - \mathbb{E}(I_{k1} \mid \mathbf{Y}, \mathbf{U}_2^\top \mathbf{W}).$$

Then

$$I_{k1} = \frac{1}{n} \text{tr} \left[(\mathbf{P}_y - l_i \mathbf{I}_n) \mathbf{W}^\top \mathbf{U}_2 \Phi^2(l_i) \mathbf{U}_2^\top \mathbf{W} (\mathbf{P}_y - l_i \mathbf{I}_n) \right] \mathbf{\Gamma}_k \mathbf{\Gamma}_k^\top + \mathcal{V}_{k1}.$$

Under the Gaussian assumption on the entries of \mathbf{W} and the orthogonality of \mathbf{U}_1 and \mathbf{U}_2 , it follows that $\mathbf{U}_1^\top \mathbf{W}$ and $\mathbf{U}_2^\top \mathbf{W}$ are independent. Moreover, by the proof of Theorem 1.1 in Bai and Silverstein (2004) [5], we have $\mathcal{V}_{k1} = O_p(n^{-1/2})$. Throughout the proof, we adopt the standard normalization that the entries of \mathbf{W} are i.i.d. $N(0, 1/n)$.

Let $\Phi(z) = (\mathbf{U}_2^\top \mathbf{W} (\mathbf{P}_y - z \mathbf{I}_n) \mathbf{W}^\top \mathbf{U}_2)^{-1}$. Note that $n\mathbf{E} = n\mathbf{U}_2^\top \mathbf{W} \mathbf{P}_y \mathbf{W}^\top \mathbf{U}_2 \sim \mathcal{W}_{p-k}(\mathbf{I}_{p-k}, q)$ and $n\mathbf{H} = n\mathbf{U}_2^\top \mathbf{W} (\mathbf{I} - \mathbf{P}_y) \mathbf{W}^\top \mathbf{U}_2 \sim \mathcal{W}_{p-k}(\mathbf{I}_{p-k}, n-q)$. Hence $\Phi(z) = ((1-z)\mathbf{E} - z\mathbf{H})^{-1}$. Consequently,

$$\begin{aligned} & \frac{1}{n} \text{tr}(\mathbf{P}_y - l_i) \mathbf{W}^\top \mathbf{U}_2 \left(\mathbf{U}_2^\top \mathbf{W} (\mathbf{P}_y - l_i) \mathbf{W}^\top \mathbf{U}_2 \right)^{-2} \mathbf{U}_2^\top \mathbf{W} (\mathbf{P}_y - l_i) \\ &= (1-l_i)^2 \frac{1}{n} \text{tr} \mathbf{E} \Phi^2(l_i) + l_i^2 \frac{1}{n} \text{tr} \mathbf{H} \Phi^2(l_i). \end{aligned}$$

Differentiating with respect to z yields

$$\begin{cases} \left(\frac{1}{n} \text{tr} \Phi(l_i) \right)' = \frac{1}{n} \text{tr} \Phi(l_i) (\mathbf{E} + \mathbf{H}) \Phi(l_i), \\ \frac{1}{n} \text{tr} \Phi(l_i) = \frac{1-l_i}{n} \text{tr} \mathbf{E} \Phi^2 - \frac{l_i}{n} \text{tr} \mathbf{H} \Phi^2(l_i), \end{cases}$$

that is,

$$\begin{cases} \frac{1}{n} \text{tr} \mathbf{E} \Phi^2(l_i) = \frac{1}{n} \text{tr} \Phi(l_i) + l_i \left(\frac{1}{n} \text{tr} \Phi(l_i) \right)', \\ \frac{1}{n} \text{tr} \mathbf{H} \Phi^2(l_i) = (1-l_i) \left(\frac{1}{n} \text{tr} \Phi(l_i) \right)' - \frac{1}{n} \text{tr} \Phi(l_i). \end{cases}$$

Therefore, it suffices to estimate the two key quantities $n^{-1} \text{tr} \Phi(l_i)$ and $(n^{-1} \text{tr} \Phi(l_i))'$.

Let $\mathcal{X}_{(p-k) \times q}$ and $\mathcal{Y}_{(p-k) \times (n-q)}$ be independent matrices with i.i.d. standard normal entries. Since

$$\Phi(z) = ((1-z)\mathbf{E} - z\mathbf{H})^{-1} = n((1-z)n\mathbf{E} - zn\mathbf{H})^{-1},$$

we have

$$\frac{1}{n}\text{tr}\Phi(z) = \frac{1}{1-z}\text{tr}\left(n\mathbf{E} - \frac{z}{1-z}n\mathbf{H}\right)^{-1}.$$

Therefore,

$$\frac{1}{n}\text{tr}\Phi(z) \stackrel{d}{=} \frac{1}{1-z}\text{tr}\left(\mathcal{X}\mathcal{X}^\top - \frac{z}{1-z}\mathcal{Y}\mathcal{Y}^\top\right)^{-1}.$$

Applying the Poincaré inequality in Lemma 2.3, we obtain the variance bound

$$\begin{aligned} & \text{Var}(\text{tr}\Phi(z)) \\ & \leq \mathbb{E}\frac{1}{n}\sum_{i=1}^{p-k}\sum_{j=1}^{n-q}\left[\frac{\partial\text{tr}\Phi(z)}{\partial\uparrow_{ij}}\right]^2 + \mathbb{E}\frac{1}{n}\sum_{i=1}^{p-k}\sum_{j=1}^q\left[\frac{\partial\text{tr}\Phi(z)}{\partial\S_{ij}}\right]^2 = O\left(\frac{p+q}{n}\right). \end{aligned} \quad (13)$$

The Poincaré inequality gives

$$\text{Var}(\text{tr}\Phi(z)) = O(1),$$

uniformly for z in a compact set away from the limiting spectral support. Hence

$$\frac{1}{n}\text{tr}\Phi(z) - \mathbb{E}\frac{1}{n}\text{tr}\Phi(z) = O_p(n^{-1}).$$

Combining this with the cumulant expansion formula in Lemma 2.2, we obtain

$$\begin{aligned} & \mathbb{E}\text{tr}(\mathcal{X}\mathcal{X}^\top(\mathcal{Y}\mathcal{Y}^\top)^{-1} - z\mathbf{I}_{p-k})^{-1} \\ & = \mathbb{E}\text{tr}\mathcal{Y}\mathcal{Y}^\top(\mathcal{X}\mathcal{X}^\top - z\mathcal{Y}\mathcal{Y}^\top)^{-1} \\ & = \mathbb{E}\frac{1}{n}\sum_{a=1}^{p-k}\sum_{b=1}^{n-q}y_{ab}\left[\mathcal{Y}^\top(\mathcal{X}\mathcal{X}^\top - z\mathcal{Y}\mathcal{Y}^\top)^{-1}\right]_{ba} \\ & = \frac{n-q}{n}\mathbb{E}\text{tr}(\mathcal{X}\mathcal{X}^\top - z\mathcal{Y}\mathcal{Y}^\top)^{-1} + \frac{z}{n}\mathbb{E}\text{tr}(\mathcal{X}\mathcal{X}^\top(\mathcal{Y}\mathcal{Y}^\top)^{-1} - z\mathbf{I}_{p-k})^{-1}\text{tr}(\mathcal{X}\mathcal{X}^\top - z\mathcal{Y}\mathcal{Y}^\top)^{-1} + O(1) \\ & = \frac{n-q}{n}\mathbb{E}\text{tr}(\mathcal{X}\mathcal{X}^\top - z\mathcal{Y}\mathcal{Y}^\top)^{-1} + \frac{z}{n}\mathbb{E}\text{tr}(\mathcal{X}\mathcal{X}^\top(\mathcal{Y}\mathcal{Y}^\top)^{-1} - z\mathbf{I}_{p-k})^{-1}\mathbb{E}\text{tr}(\mathcal{X}\mathcal{X}^\top - z\mathcal{Y}\mathcal{Y}^\top)^{-1} + O(1), \end{aligned}$$

where the last equality follows from the Cauchy–Schwarz inequality. Consequently,

$$\begin{aligned} & \left| \mathbb{E}\frac{1}{n}\text{tr}(\mathcal{X}\mathcal{X}^\top(\mathcal{Y}\mathcal{Y}^\top)^{-1} - z\mathbf{I})^{-1}\text{tr}(\mathcal{X}\mathcal{X}^\top - z\mathcal{Y}\mathcal{Y}^\top)^{-1} \right. \\ & \quad \left. - \mathbb{E}\frac{1}{n}\text{tr}(\mathcal{X}\mathcal{X}^\top(\mathcal{Y}\mathcal{Y}^\top)^{-1} - z\mathbf{I})^{-1}\mathbb{E}\text{tr}(\mathcal{X}\mathcal{X}^\top - z\mathcal{Y}\mathcal{Y}^\top)^{-1} \right| \\ & = \left| \mathbb{E}(1 - \mathbb{E})\frac{1}{n}\text{tr}(\mathcal{X}\mathcal{X}^\top(\mathcal{Y}\mathcal{Y}^\top)^{-1} - z\mathbf{I})^{-1}(1 - \mathbb{E})\text{tr}(\mathcal{X}\mathcal{X}^\top - z\mathcal{Y}\mathcal{Y}^\top)^{-1} \right| \\ & \leq \sqrt{\mathbb{E}\left|(1 - \mathbb{E})\frac{1}{n}\text{tr}(\mathcal{X}\mathcal{X}^\top(\mathcal{Y}\mathcal{Y}^\top)^{-1} - z\mathbf{I})^{-1}\right|^2} \sqrt{\mathbb{E}\left|(1 - \mathbb{E})\text{tr}(\mathcal{X}\mathcal{X}^\top - z\mathcal{Y}\mathcal{Y}^\top)^{-1}\right|^2} \\ & \leq O\left(\frac{1}{n}\right). \end{aligned}$$

Here the replacement of $\mathbb{E}(\text{tr}\mathbf{A} \text{tr}\mathbf{B})$ by $\mathbb{E}\text{tr}\mathbf{A} \mathbb{E}\text{tr}\mathbf{B}$ introduces an $O(1)$ error, since by the Poincaré inequality both $\text{Var}(\text{tr}\mathbf{A})$ and $\text{Var}(\text{tr}\mathbf{B})$ are uniformly bounded, and hence the covariance is $O(1)$. After dividing by n , this error becomes $O(1/n)$.

It follows that

$$\mathbb{E}\text{tr}(\mathcal{X}\mathcal{X}^\top - z\mathcal{Y}\mathcal{Y}^\top)^{-1} = \frac{\mathbb{E}\text{tr}(\mathcal{X}\mathcal{X}^\top(\mathcal{Y}\mathcal{Y}^\top)^{-1} - z\mathbf{I})^{-1}}{\frac{n-q}{n} + \frac{z}{n}\mathbb{E}\text{tr}(\mathcal{X}\mathcal{X}^\top(\mathcal{Y}\mathcal{Y}^\top)^{-1} - z\mathbf{I})^{-1}} + O(1),$$

and hence

$$\begin{aligned} \frac{1}{n}\text{tr}\Phi(z) &= \frac{1}{1-z} \frac{\frac{1}{n}\mathbb{E}\text{tr}\left(\mathcal{X}\mathcal{X}^\top(\mathcal{Y}\mathcal{Y}^\top)^{-1} - \frac{z}{1-z}\mathbf{I}\right)^{-1}}{\frac{n-q}{n} + \frac{z}{1-z}\frac{1}{n}\mathbb{E}\text{tr}\left(\mathcal{X}\mathcal{X}^\top(\mathcal{Y}\mathcal{Y}^\top)^{-1} - \frac{z}{1-z}\mathbf{I}\right)^{-1}} + O_p\left(\frac{1}{n}\right) \\ &= \frac{1}{z} \frac{-c_1 + (1-z)s(z)}{1 - c_2 - c_1 + (1-z)s(z)} + O_p\left(\frac{1}{n}\right) \\ &:= QQ_1(z) + O_p\left(\frac{1}{n}\right). \end{aligned} \quad (14)$$

Since $n^{-1}\text{tr}\Phi(z)$ is analytic on $\mathbb{C} \setminus \mathbb{R}$ and converges to its deterministic limit uniformly on compact subsets of a neighborhood of l_i (by standard resolvent convergence results for the Fisher-type matrix), Cauchy's integral formula implies that the derivatives also converge, and thus the limit and differentiation can be interchanged:

$$\lim_{n \rightarrow \infty} \frac{\partial}{\partial z} \mathbb{E} \frac{1}{n} \text{tr}\Phi(z) = \frac{\partial}{\partial z} \lim_{n \rightarrow \infty} \mathbb{E} \frac{1}{n} \text{tr}\Phi(z).$$

Therefore,

$$\begin{aligned} \left(\frac{1}{n}\text{tr}\Phi(z)\right)' &= \frac{d}{dz} \left(\frac{1}{z} \frac{-c_1 + (1-z)s(z)}{1 - c_2 - c_1 + (1-z)s(z)}\right) + O_p\left(\frac{1}{\sqrt{n}}\right) \\ &= \frac{1}{z^2} \frac{c_1 - (1-z)s(z)}{1 - c_1 - c_2 + (1-z)s(z)} + \frac{(1-c_2)(-s(z) + (1-z)s'(z))}{z(1 - c_1 - c_2 + (1-z)s(z))^2} + O_p\left(\frac{1}{\sqrt{n}}\right) \\ &:= QQ_2(z) + O_p\left(\frac{1}{\sqrt{n}}\right). \end{aligned} \quad (15)$$

The above resolvent estimates hold uniformly for z in a fixed neighborhood of γ_i that stays away from the limiting spectral support. Since r_i is spike, $l_i - \gamma_i = O_p(n^{-1/2})$. Therefore, by the resolvent identity and Taylor expansion of the deterministic limits, these estimates may be evaluated at the random point $z = l_i$, with an additional error of order $O_p(n^{-1/2})$. Consequently, combining (14) and (15) yields

$$\begin{aligned} QQ_1(l_i) &= \frac{-c_1 r_i ((1-c_2)r_i + c_2)}{r_i(\eta r_i - \omega) - (\eta r_i - \omega)^2(1-r_i)} + O_p\left(\frac{1}{\sqrt{n}}\right) \\ &:= F_1(r_i) + O_p\left(\frac{1}{\sqrt{n}}\right), \end{aligned} \quad (16)$$

$$\begin{aligned}
QQ_2(l_i) &= \frac{r_i^2 (\omega(1-c_2)r_i((1-c_1)r_i+c_1) + c_1(\eta r_i - \omega)(\eta r_i^2 - \omega))}{((1-c_1)r_i+c_1)^2((1-c_2)r_i+c_2)(\eta r_i - \omega)^2(\eta r_i^2 - \omega)} + O_p\left(\frac{1}{\sqrt{n}}\right) \\
&:= F_2(r_i) + O_p\left(\frac{1}{\sqrt{n}}\right), \tag{17}
\end{aligned}$$

$$\frac{1}{n} \text{tr} \mathbf{E} \Phi^2(l_i) = \frac{\omega(1-c_2)r_i^2}{(\eta r_i - \omega)^2(\eta r_i^2 - \omega)} + O_p\left(\frac{1}{\sqrt{n}}\right), \tag{18}$$

$$\frac{1}{n} \text{tr} \mathbf{H} \Phi^2(l_i) = \frac{c_1 r_i^2}{(\eta r_i^2 - \omega)((1-c_1)r_i+c_1)^2} + O_p\left(\frac{1}{\sqrt{n}}\right). \tag{19}$$

Here $\eta = (1-c_1)(1-c_2)$ and $\omega = c_1 c_2$. Substituting these expansions into I_{k1} yields

$$\begin{aligned}
I_{k1} &= \left((1-l_i)^2 \frac{1}{n} \text{tr} \mathbf{E} \Phi^2(l_i) + l_i^2 \frac{1}{n} \text{tr} \mathbf{H} \Phi^2(l_i) \right) \mathbf{\Gamma}_k \mathbf{\Gamma}_k^\top + \mathcal{V}_{k1} \\
&= \left((1-2l_i) \frac{1}{n} \text{tr} \Phi(l_i) + l_i(1-l_i) \left(\frac{1}{n} \text{tr} \Phi(l_i) \right)' \right) \mathbf{\Gamma}_k \mathbf{\Gamma}_k^\top + \mathcal{V}_{k1} \\
&= ((1-2l_i)QQ_1(l_i) + l_i(1-l_i)QQ_2(l_i)) \times \mathbf{\Gamma}_k \mathbf{\Gamma}_k^\top + O_p\left(\frac{1}{\sqrt{n}}\right). \tag{20}
\end{aligned}$$

We next analyze I_{k2} . Let $\mathbf{Y} = \mathbf{U}_y \mathbf{\Lambda}_y \mathbf{V}_y$. Following the treatment in Bao et al. (2019) [8], since \mathbf{Y} has i.i.d. Gaussian entries, in its SVD the left singular vectors \mathbf{U}_y are Haar distributed on the orthogonal group and are independent of $(\mathbf{\Lambda}_y, \mathbf{V}_y)$. Let $\tilde{\mathbf{U}}_y$ be an independent Haar orthogonal matrix with the same dimension as \mathbf{U}_y . Then replacing \mathbf{U}_y by $\tilde{\mathbf{U}}_y$ does not change the distribution of I_{k2}, I_{k3}, I_{k4} . Accordingly, I_{k2} can be decomposed as

$$\begin{aligned}
I_{k2} &= \mathbf{\Lambda}_k \mathbf{V}_1^\top \tilde{\mathbf{U}}_y \mathbf{\Lambda}_y \mathbf{V}_y^\top (\mathbf{P}_y - l_i \mathbf{I}_n) \mathbf{W}^\top \mathbf{U}_2 (\mathbf{U}_2^\top \mathbf{W} (\mathbf{P}_y - l_i \mathbf{I}_n) \mathbf{W}^\top \mathbf{U}_2)^{-2} \\
&\quad \times \mathbf{U}_2^\top \mathbf{W} (\mathbf{P}_y - l_i \mathbf{I}_n) \mathbf{V}_y \mathbf{\Lambda}_y \tilde{\mathbf{U}}_y^\top \mathbf{V}_1 \mathbf{\Lambda}_k + O_p\left(\frac{\log n}{n}\right) \\
&= \frac{1}{q} \text{tr} \mathbf{\Lambda}_y \mathbf{V}_y^\top (\mathbf{P}_y - l_i \mathbf{I}_n) \mathbf{W}^\top \mathbf{U}_2 (\mathbf{U}_2^\top \mathbf{W} (\mathbf{P}_y - l_i \mathbf{I}_n) \mathbf{W}^\top \mathbf{U}_2)^{-2} \\
&\quad \times \mathbf{U}_2^\top \mathbf{W} (\mathbf{P}_y - l_i \mathbf{I}_n) \mathbf{V}_y \mathbf{\Lambda}_y \times \mathbf{\Lambda}_k \mathbf{\Lambda}_k^\top + O_p\left(\frac{\log n}{n}\right) \\
&:= (1-l_i)^2 \frac{1}{q} \text{tr} \mathbf{Y} \mathbf{W}^\top \mathbf{U}_2 \Phi(l_i)^2 \mathbf{U}_2^\top \mathbf{W} \mathbf{Y}^\top \times \mathbf{\Lambda}_k \mathbf{\Lambda}_k^\top + \mathcal{V}_{k2} + O_p\left(\frac{\log n}{n}\right). \tag{21}
\end{aligned}$$

By the Poincaré inequality, the variance of the normalized trace $q^{-1} \text{tr} \mathbf{Y} \mathbf{W}^\top \mathbf{U}_2 \Phi(l_i)^2 \mathbf{U}_2^\top \mathbf{W} \mathbf{Y}^\top$ is uniformly bounded, which is analogous to (13). Using the cumulant expansion, we obtain

$$\begin{aligned}
&\mathbb{E} \text{tr} \mathbf{Y} \mathbf{W}^\top \mathbf{U}_2 \Phi(l_i)^2 \mathbf{U}_2^\top \mathbf{W} \mathbf{Y}^\top \\
&= \mathbb{E} \frac{q}{n} \text{tr} (\mathbf{E} + \mathbf{H}) \Phi^2(l_i) - \mathbb{E} \frac{1}{n} \left(\text{tr} \mathbf{H} \Phi(l_i) \text{tr} \mathbf{E} \Phi^2(l_i) + \text{tr} \mathbf{E} \Phi(l_i) \text{tr} \mathbf{H} \Phi^2(l_i) \right) + O\left(\frac{q}{n}\right),
\end{aligned}$$

and hence

$$\begin{aligned}
&\mathbb{E} \frac{1}{n} \text{tr} \mathbf{Y} \mathbf{W}^\top \mathbf{U}_2 \Phi(l_i)^2 \mathbf{U}_2^\top \mathbf{W} \mathbf{Y}^\top \\
&= \mathbb{E} \frac{q}{n} \frac{1}{n} \text{tr} (\mathbf{E} + \mathbf{H}) \Phi^2(l_i) - \mathbb{E} \frac{1}{n} \text{tr} \mathbf{H} \Phi(l_i) \frac{1}{n} \text{tr} \mathbf{E} \Phi^2(l_i) - \mathbb{E} \frac{1}{n} \text{tr} \mathbf{E} \Phi(l_i) \frac{1}{n} \text{tr} \mathbf{H} \Phi^2(l_i) + O\left(\frac{q}{n^2}\right)
\end{aligned}$$

$$= \mathbb{E} \frac{q}{n} \frac{1}{n} \text{tr}(\mathbf{E} + \mathbf{H}) \Phi^2(l_i) - \mathbb{E} \frac{1}{n} \text{tr} \mathbf{H} \Phi(l_i) \mathbb{E} \frac{1}{n} \text{tr} \mathbf{E} \Phi^2(l_i) - \mathbb{E} \frac{1}{n} \text{tr} \mathbf{E} \Phi(l_i) \mathbb{E} \frac{1}{n} \text{tr} \mathbf{H} \Phi^2(l_i) + O\left(\frac{q}{n^2}\right).$$

By the same argument as for I_{k1} , we further obtain

$$\begin{aligned} & \frac{1}{n} \text{tr} \mathbf{Y} \mathbf{W} \mathbf{W}^\top \mathbf{U}_2 \Phi(l_i)^2 \mathbf{U}_2^\top \mathbf{W} \mathbf{Y} \\ &= \left(\frac{c_1}{l_i} - \frac{1-l_i}{l_i} s(l_i) + s(l_i) \right) \frac{1}{n} \text{tr} \Phi(l_i) \\ & \quad + (c_1 + c_2 - 2(1-l_i)s(l_i)) \left(\frac{1}{n} \text{tr} \Phi(l_i) \right)' + O_p\left(\frac{1}{\sqrt{n}}\right) \\ &= \left(\frac{c_1}{l_i} - \frac{1-l_i}{l_i} s(l_i) + s(l_i) \right) QQ_1(l_i) + (c_1 + c_2 - 2(1-l_i)s(l_i)) QQ_2(l_i) + O_p\left(\frac{1}{\sqrt{n}}\right). \end{aligned}$$

Therefore, the asymptotic expansion of I_{k2} is

$$\begin{aligned} I_{k2} &= \frac{(1-l_i)^2}{c_2} \left(\frac{c_1 - (1-2l_i)s(l_i)}{l_i} QQ_1(l_i) + (c_1 + c_2 - 2(1-l_i)s(l_i)) QQ_2(l_i) \right) \\ & \quad \times \mathbf{\Lambda}_k \mathbf{\Lambda}_k^\top + O_p\left(\frac{1}{\sqrt{n}}\right). \end{aligned} \tag{22}$$

For the cross terms I_{k3} and I_{k4} , conditional on $\mathbf{U}_2^\top \mathbf{W}$ and \mathbf{Y} , they can be viewed as linear combinations of Gaussian random variables. Using the boundedness of the operator norm,

$$\left\| \mathbf{V}_1^\top \mathbf{Y} (\mathbf{P}_y - l_i) \mathbf{W}^\top \mathbf{U}_2 \Phi(l_i)^2 \mathbf{U}_2^\top \mathbf{W} (\mathbf{P}_y - l_i)^2 \mathbf{W}^\top \mathbf{U}_2 \Phi(l_i)^2 \mathbf{U}_2^\top \mathbf{W} (\mathbf{P}_y - l_i) \mathbf{Y}^\top \mathbf{V}_1 \right\| = O(1),$$

Since k is fixed, this gives the entrywise bounds

$$[I_{k3}]_{ab} = O_p(n^{-1/2}), \quad [I_{k4}]_{ab} = O_p(n^{-1/2}), \quad 1 \leq a, b \leq k.$$

In particular,

$$[I_{k3}]_{ii} = O_p(n^{-1/2}), \quad [I_{k4}]_{ii} = O_p(n^{-1/2}).$$

It remains to control the off-diagonal entries. We explain the argument for I_{k1} , the other terms are handled in the same way. Conditional on \mathbf{Y} and $\mathbf{U}_2^\top \mathbf{W}$, the rows of $\mathbf{U}_1^\top \mathbf{W}$ are independent centered Gaussian vectors and are independent of $\mathbf{U}_2^\top \mathbf{W}$. Hence, for $a \neq b$,

$$\mathbb{E} \left([I_{k1}]_{ab} \mid \mathbf{Y}, \mathbf{U}_2^\top \mathbf{W} \right) = 0.$$

Moreover, by the resolvent bound $\|\mathbf{D}^{-1}\| = O_p(1)$ and the fact that k is fixed, the corresponding conditional variance satisfies

$$\text{Var} \left([I_{k1}]_{ab} \mid \mathbf{Y}, \mathbf{U}_2^\top \mathbf{W} \right) = O_p(n^{-1}).$$

Therefore,

$$[I_{k1}]_{ab} = O_p(n^{-1/2}), \quad a \neq b.$$

For I_{k2} , after the Haar replacement of the left singular vectors of \mathbf{Y} , the off-diagonal entries

have conditional mean zero and conditional variance $O_p(n^{-1})$. Thus

$$[I_{k2}]_{ab} = O_p(n^{-1/2}), \quad a \neq b.$$

Similarly, the cross terms I_{k3} and I_{k4} are conditionally centered Gaussian bilinear forms with conditional variances of order n^{-1} . Hence

$$[I_{k3}]_{ab} = O_p(n^{-1/2}), \quad [I_{k4}]_{ab} = O_p(n^{-1/2}), \quad a \neq b.$$

Combining these bounds gives

$$[\mathbf{M}_i]_{ab} = O_p(n^{-1/2}), \quad a \neq b.$$

Since k is fixed and the diagonal entries of \mathbf{M}_i are $O_p(1)$, it follows that

$$\|\mathbf{M}_i\| = O_p(1).$$

This completes the proof of Lemma 5.1. \square

Proof of Lemma 5.2. We first justify the joint Gaussian convergence of the fluctuation terms. By the Cramér–Wold device, it is enough to consider an arbitrary fixed linear combination

$$T_n = a_1 X_{1n} + a_2 X_{2n} + a_3 X_{3n}, \quad a_1, a_2, a_3 \in \mathbb{R}.$$

The terms X_{1n} , X_{2n} , and X_{3n} can be represented, up to negligible errors, as centered quadratic and bilinear forms with random coefficient matrices that are independent of the leading Gaussian variables after conditioning on \mathbf{Y} and $\mathbf{U}_2^\top \mathbf{W}$. These coefficient matrices are uniformly bounded in operator norm with probability tending to one, and the normalized trace quantities appearing in their variance formulas have deterministic limits. Therefore, by the central limit theorem for random sesquilinear forms in Bai and Yao (2008) [2], every fixed linear combination of X_{1n} , X_{2n} , and X_{3n} has an asymptotically normal distribution. Since the coefficients in the linear combination are arbitrary, the Cramér–Wold device implies the joint Gaussian convergence of (X_{1n}, X_{2n}, X_{3n}) .

It remains to compute the limiting variances and covariances, which determine the variance of the final linear combination appearing in $G_{i,n}$. These are obtained as follows. We next study the fluctuation behavior of the i -th diagonal entry $[\mathbf{M}_i]_{jj}$. Since the entries of the random matrices \mathcal{V}_{k1} and \mathcal{V}_{k2} are quadratic forms, their variances can be derived from Bai and Yao (2008) [2]:

$$\begin{aligned} \text{Var}([\sqrt{n}\mathcal{V}_{k1}]_{jj}) &= \mathbb{E} \frac{2(1-r_i)^2}{n} \text{tr}(\mathbf{P}_y - l_i \mathbf{I}_n) \mathbf{W}^\top \mathbf{U}_2 \Phi^2(l_i) \mathbf{U}_2^\top \mathbf{W} (\mathbf{P}_y - l_i \mathbf{I}_n)^2 \\ &\quad \times \mathbf{W}^\top \mathbf{U}_2 \Phi^2(l_i) \mathbf{U}_2^\top \mathbf{W} (\mathbf{P}_y - l_i \mathbf{I}_n), \\ \text{Var}([\sqrt{n}\mathcal{V}_{k2}]_{jj}) &= \mathbb{E} (1-l_i)^4 \frac{2r_i^2}{q} \text{tr} \mathbf{Y} \mathbf{W}^\top \mathbf{U}_2 \Phi^2(l_i) \mathbf{U}_2^\top \mathbf{W} \mathbf{Y}^\top \mathbf{Y} \mathbf{W}^\top \mathbf{U}_2 \Phi^2(l_i) \mathbf{U}_2^\top \mathbf{W} \mathbf{Y}^\top. \end{aligned}$$

Using the matrix identity $(\mathbf{E} + \mathbf{H})\Phi(z) = z^{-1}(\mathbf{E}\Phi - \mathbf{I}_{p-k})$, we may rewrite the variance of \mathcal{V}_{k1}

into the limiting forms of three expectation terms:

$$\begin{aligned}
\text{Var}([\sqrt{n}\mathcal{V}_{k1}]_{jj}) &= \mathbb{E} \frac{2(1-r_i)^2}{n} \text{tr} \Phi^2(l_i) \mathbf{U}_2^\top \mathbf{W} (\mathbf{P}_y - l_i \mathbf{I}_n)^2 \mathbf{W}^\top \mathbf{U}_2 \Phi^2(l_i) \mathbf{U}_2^\top \mathbf{W} (\mathbf{P}_y - l_i \mathbf{I}_n)^2 \mathbf{W}^\top \mathbf{U}_2 \\
&= \mathbb{E} \frac{2(1-r_i)^2}{n} \text{tr} \Phi^2(l_i) ((1-l_i)^2 \mathbf{E} + l_i^2 \mathbf{H}) \Phi^2(l_i) ((1-l_i)^2 \mathbf{E} + l_i^2 \mathbf{H}) \\
&= \mathbb{E} \frac{2(1-r_i)^2}{n} \text{tr} ((1-l_i) \mathbf{E} \Phi(l_i) - l_i \mathbf{I}) \Phi(l_i) ((1-l_i) \mathbf{E} \Phi(l_i) - l_i \mathbf{I}) \Phi(l_i) \\
&= 2(1-r_i)^2 \left((1-l_i)^2 \mathbb{E} \frac{1}{n} \text{tr} \mathbf{E} \Phi^2(l_i) \mathbf{E} \Phi^2(l_i) \right. \\
&\quad \left. - 2(1-l_i) l_i \mathbb{E} \frac{1}{n} \text{tr} \mathbf{E} \Phi^3(l_i) + \mathbb{E} \frac{l_i^2}{n} \text{tr} \Phi^2(l_i) \right). \tag{23}
\end{aligned}$$

This shows that the limiting variance of $\sqrt{n}\mathcal{V}_{k1}$ reduces to the limits of the three expectation terms in (23).

We now turn to

$$\text{Var}([\sqrt{n}\mathcal{V}_{k2}]_{jj}) = \mathbb{E} \frac{2r_i^2(1-l_i)^4}{q} \text{tr} \mathbf{Y} \mathbf{W}^\top \mathbf{U}_2 \Phi^2(l_i) \mathbf{U}_2^\top \mathbf{W} \mathbf{Y}^\top \mathbf{Y} \mathbf{W}^\top \mathbf{U}_2 \Phi^2(l_i) \mathbf{U}_2^\top \mathbf{W} \mathbf{Y}^\top.$$

Expanding this variance via the cumulant expansion yields

$$\begin{aligned}
&\mathbb{E} \frac{1}{q} \text{tr} \mathbf{Y} \mathbf{W}^\top \mathbf{U}_2 \Phi^2(l_i) \mathbf{U}_2^\top \mathbf{W} \mathbf{Y}^\top \mathbf{Y} \mathbf{W}^\top \mathbf{U}_2 \Phi^2(l_i) \mathbf{U}_2^\top \mathbf{W} \mathbf{Y}^\top \\
&= -\mathbb{E} \frac{1}{n} \text{tr} \mathbf{H} \Phi(l_i) \frac{1}{q} \text{tr} \mathbf{E} \Phi^2(l_i) \mathbf{U}_2^\top \mathbf{W} \mathbf{Y}^\top \mathbf{Y} \mathbf{W}^\top \mathbf{U}_2 \Phi^2(l_i) \\
&\quad - \mathbb{E} \frac{1}{n} \text{tr} \mathbf{H} \Phi^2(l_i) \frac{1}{q} \text{tr} \mathbf{E} \Phi(l_i) \mathbf{U}_2^\top \mathbf{W} \mathbf{Y}^\top \mathbf{Y} \mathbf{W}^\top \mathbf{U}_2 \Phi^2(l_i) \\
&\quad + \mathbb{E} \frac{1}{n} \text{tr} \mathbf{E} \Phi^2(l_i) \frac{1}{q} \text{tr} \mathbf{U}_2^\top \mathbf{W} \mathbf{Y}^\top \mathbf{Y} \mathbf{W}^\top \mathbf{U}_2 \Phi^2(l_i) \\
&\quad - \mathbb{E} \frac{1}{q} \text{tr} \mathbf{H} \Phi^2(l_i) \mathbf{U}_2^\top \mathbf{W} \mathbf{Y}^\top \mathbf{Y} \mathbf{W}^\top \mathbf{U}_2 \Phi(l_i) \frac{1}{n} \text{tr} \mathbf{E} \Phi^2(l_i) \\
&\quad - \mathbb{E} \frac{1}{q} \text{tr} \mathbf{H} \Phi^2(l_i) \mathbf{U}_2^\top \mathbf{W} \mathbf{Y}^\top \mathbf{Y} \mathbf{W}^\top \mathbf{U}_2 \Phi^2(l_i) \frac{1}{n} \text{tr} \mathbf{E} \Phi(l_i) + O\left(\frac{1}{n}\right) \\
&= J_{k1}(r_i) + J_{k2}(r_i) + J_{k3}(r_i) + J_{k4}(r_i) + J_{k5}(r_i) + O\left(\frac{1}{n}\right).
\end{aligned}$$

Indeed, each normalized trace term is a smooth function of Gaussian entries with gradient of order $O(n^{-1})$, so the Gaussian Poincaré inequality implies the variances of the above trace terms are of order $O(n^{-2})$. Using the previously obtained estimates for $n^{-1} \text{tr} \mathbf{E} \Phi$, $n^{-1} \text{tr} \mathbf{H} \Phi$, $n^{-1} \text{tr} \mathbf{E} \Phi^2$, and $n^{-1} \text{tr} \mathbf{H} \Phi^2$, and controlling the approximation errors via the Cauchy–Schwarz inequality, it remains to compute the limits of three key quantities stated in Lemma 6.1:

$$\begin{aligned}
&\frac{1}{q} \text{tr} \mathbf{U}_2^\top \mathbf{W} \mathbf{Y}^\top \mathbf{Y} \mathbf{W}^\top \mathbf{U}_2 \Phi^2(l_i), \quad \frac{1}{q} \text{tr} \mathbf{E} \Phi^2(l_i) \mathbf{U}_2^\top \mathbf{W} \mathbf{Y}^\top \mathbf{Y} \mathbf{W}^\top \mathbf{U}_2 \Phi^2(l_i), \\
&\frac{1}{q} \text{tr} \mathbf{H} \Phi^2(l_i) \mathbf{U}_2^\top \mathbf{W} \mathbf{Y}^\top \mathbf{Y} \mathbf{W}^\top \mathbf{U}_2 \Phi^2(l_i).
\end{aligned}$$

Lemma 6.1 (Resolvent trace estimates). *Under the same conditions as in Theorem 2.4, the following estimates hold:*

$$\begin{aligned}\mathbb{E}\frac{1}{n}\text{tr}\Phi^2(l_i) &= \frac{c_1(1-c_2)r_i^4}{((1-c_1)r_i+c_1)^2(\eta r_i-\omega)^2(\eta r_i^2-\omega)} + O\left(\frac{1}{\sqrt{n}}\right) \\ &:= P_1(r_i) + O\left(\frac{1}{\sqrt{n}}\right),\end{aligned}\tag{24}$$

$$\mathbb{E}\frac{1}{n}\text{tr}\mathbf{E}\Phi^3(l_i) = F_3(r_i) + O\left(n^{-\frac{1}{4}}\right),\tag{25}$$

$$\mathbb{E}\frac{1}{n}\text{tr}\mathbf{E}\Phi^2(l_i)\mathbf{E}\Phi^2(l_i) = Q_3(r_i) + O\left(n^{-\frac{1}{6}}\right),\tag{26}$$

$$\mathbb{E}\frac{1}{q}\text{tr}\mathbf{Y}\mathbf{W}^\top\mathbf{U}_2\Phi^2(l_i)\mathbf{E}\Phi^2(l_i)\mathbf{U}_2^\top\mathbf{W}\mathbf{Y}^\top = \frac{Q_4(r_i)}{c_2} + O\left(n^{-\frac{1}{6}}\right),\tag{27}$$

$$\mathbb{E}\frac{1}{q}\text{tr}\mathbf{Y}\mathbf{W}^\top\mathbf{U}_2\Phi^2(l_i)\mathbf{E}\Phi(l_i)\mathbf{U}_2^\top\mathbf{W}\mathbf{Y}^\top = \frac{Q_5(r_i)}{c_2} + O\left(n^{-\frac{1}{4}}\right),\tag{28}$$

$$\mathbb{E}\frac{1}{q}\text{tr}\mathbf{Y}\mathbf{W}^\top\mathbf{U}_2\Phi^3(l_i)\mathbf{U}_2^\top\mathbf{W}\mathbf{Y}^\top = \frac{Q_7(r_i)}{c_2} + O\left(n^{-\frac{1}{8}}\right),\tag{29}$$

For notational convenience, the definitions of $F_3(r_i)$, $Q_3(r_i)$, $Q_4(r_i)$, $Q_5(r_i)$, and $Q_7(r_i)$ are given in (36), (37), (38), (39), and (40), respectively.

The detailed proof of Lemma 6.1 is deferred to Section 7.

For the cross terms I_{k3} and I_{k4} , one has $I_{k3} + I_{k4} = o_p(1)$. Moreover, their fluctuation can be quantified as follows:

$$I_{k3} + I_{k4} = 2(1-l_i)\Gamma_k\mathbf{U}_1^\top\mathbf{W}(\mathbf{P}_y-l_i\mathbf{I}_n)\mathbf{W}^\top\mathbf{U}_2\Phi^2(l_i)\mathbf{U}_2^\top\mathbf{W}\mathbf{V}_y^\top\Lambda_y\tilde{\mathbf{U}}_y\Lambda_k,$$

where $\mathbf{U}_1^\top\mathbf{W}$ and the Haar matrix $\tilde{\mathbf{U}}_y$ are independent of

$$\mathcal{B} = (\mathbf{P}_y - l_i\mathbf{I}_n)\mathbf{W}^\top\mathbf{U}_2\Phi^2(l_i)\mathbf{U}_2^\top\mathbf{W}\mathbf{V}_y^\top\Lambda_y.$$

Therefore,

$$\begin{aligned}&\text{Var}(\sqrt{n}[I_{k3} + I_{k4}]_{jj}) \\ &= 4(1-l_i)^2(1-r_i)r_i\mathbb{E}\frac{1}{q}\text{tr}\mathcal{B}\mathcal{B}^\top \\ &= 4(1-l_i)^3(1-r_i)r_i\mathbb{E}\frac{1}{q}\text{tr}\mathbf{Y}\mathbf{W}^\top\mathbf{U}_2\Phi^2(l_i)\mathbf{E}\Phi^2(l_i)\mathbf{U}_2^\top\mathbf{W}\mathbf{Y}^\top \\ &\quad + 4(1-l_i)^2(1-r_i)r_i\mathbb{E}\frac{p}{n}\frac{1}{q}\text{tr}\mathbf{Y}\mathbf{W}^\top\mathbf{U}_2\Phi^3(l_i)\mathbf{U}_2^\top\mathbf{W}\mathbf{Y}^\top \\ &= \frac{4(\eta r_i - \omega)^3(1-r_i)^4Q_4(r_i)}{c_2r_i^2} + \frac{4c_1(\eta r_i - \omega)^2(1-r_i)^3Q_7(r_i)}{c_2r_i} + O(n^{-1/8}).\end{aligned}$$

Combining (23) with (24)–(26) yields

$$\begin{aligned}\text{Var}([\sqrt{n}\mathcal{V}_{k1}]_{jj}) &= 2(1-r_i)^2 P_1(r_i) - 4\frac{\eta r_i - \omega}{r_i}(1-r_i)^3(P_1(r_i) + F_3(r_i)) \\ &\quad + \frac{2(\eta r_i - \omega)^2}{r_i^2}(1-r_i)^4(P_1(r_i) + 2F_3(r_i) + Q_3(r_i)) \\ &\quad + O\left(n^{-1/16}\right),\end{aligned}\tag{30}$$

where the explicit expressions of $P_1(r_i)$, $F_3(r_i)$, and $Q_3(r_i)$ are given in (24), (36), and (37), respectively.

We next compute $\text{Var}([\sqrt{n}\mathcal{V}_{k2}]_{jj})$. Further derivations yield

$$J_{k1}(r_i) = \frac{c_1 r_i + \omega(1-r_i)}{c_2 r_i - c_2(\eta r_i - \omega)(1-r_i)} Q_4(r_i),\tag{31}$$

$$J_{k2}(r_i) = \frac{-c_1 r_i^2 Q_5(r_i)}{c_2(\eta r_i^2 - \omega)((1-c_1)r_i + c_1)^2},\tag{32}$$

where $Q_4(r_i)$ and $Q_5(r_i)$ are defined in (38) and (39).

Next, the term $n^{-1}\text{tr}\mathbf{U}_2^\top \mathbf{WY}^\top \mathbf{YW}^\top \mathbf{U}_2 \Phi^2(l_i) = n^{-1}\text{tr}\mathbf{YW}^\top \mathbf{U}_2 \Phi^2(l_i) \mathbf{U}_2^\top \mathbf{WY}^\top$ appearing in J_{k3} has already been computed in the analysis of I_{k2} , and thus

$$\begin{aligned}J_{k3}(r_i) &= \frac{\omega(1-c_2)r_i^2}{c_2(\eta r_i - \omega)^2(\eta r_i^2 - \omega)} \left(\left(\frac{c_1 r_i + \omega(1-r_i)}{r_i - (\eta r_i - \omega)(1-r_i)} - \frac{\omega}{\eta r_i - \omega} \right) F_1(r_i) \right. \\ &\quad \left. + (c_1 + c_2 + \frac{\omega(1-r_i)}{r_i}) F_2(r_i) \right).\end{aligned}\tag{33}$$

Finally, we simplify J_{k4} and J_{k5} . Note that

$$\begin{aligned}\frac{1}{n}\text{tr}\mathbf{H}\Phi^2(l_i) \mathbf{U}_2^\top \mathbf{WY}^\top \mathbf{YW}^\top \mathbf{U}_2 \Phi(l_i) &= \frac{1-l_i}{l_i} \frac{1}{n}\text{tr}\mathbf{E}\Phi^2(l_i) \mathbf{U}_2^\top \mathbf{WY}^\top \mathbf{YW}^\top \mathbf{U}_2 \Phi(l_i) \\ &\quad - \frac{1}{l_i n}\text{tr}\Phi(l_i) \mathbf{U}_2^\top \mathbf{WY}^\top \mathbf{YW}^\top \mathbf{U}_2 \Phi(l_i), \\ \frac{1}{n}\text{tr}\mathbf{H}\Phi^2(l_i) \mathbf{U}_2^\top \mathbf{WY}^\top \mathbf{YW}^\top \mathbf{U}_2 \Phi^2(l_i) &= \frac{1-l_i}{l_i} \frac{1}{n}\text{tr}\mathbf{E}\Phi^2(l_i) \mathbf{U}_2^\top \mathbf{WY}^\top \mathbf{YW}^\top \mathbf{U}_2 \Phi^2(l_i) \\ &\quad - \frac{1}{l_i n}\text{tr}\Phi(l_i) \mathbf{U}_2^\top \mathbf{WY}^\top \mathbf{YW}^\top \mathbf{U}_2 \Phi^2(l_i),\end{aligned}$$

which leads to

$$\begin{aligned}J_{k4}(r_i) &= -\frac{\omega(1-c_2)r_i^2}{(\eta r_i - \omega)^2(\eta r_i^2 - \omega)} \left(\frac{(\eta r_i - \omega)(1-r_i)}{c_2(r_i - (\eta r_i - \omega)(1-r_i))} Q_5(r_i) \right. \\ &\quad \left. - \frac{((c_1 r_i + \omega(1-r_i))/(r_i - (\eta r_i - \omega)(1-r_i)) - \omega/(\eta r_i - \omega)) F_1(r_i)}{c_2(r_i - (\eta r_i - \omega)(1-r_i))/r_i} \right. \\ &\quad \left. + \frac{(c_1 + c_2 + \omega(1-r_i)/r_i) F_2(r_i)}{c_2(r_i - (\eta r_i - \omega)(1-r_i))/r_i} \right)\end{aligned}$$

$$\begin{aligned}
&= -\frac{\omega(1-c_2)r_i^2}{(\eta r_i - \omega)^2(\eta r_i^2 - \omega)} \left(\frac{(\eta r_i - \omega)(1-r_i)}{c_2(r_i - (\eta r_i - \omega)(1-r_i))} Q_5(r_i) \right. \\
&\quad \left. - \frac{r_i \left((c_1 r_i + \omega(1-r_i))(\eta r_i - \omega) - \omega(r_i - (\eta r_i - \omega)(1-r_i)) \right) F_1(r_i)}{c_2(r_i - (\eta r_i - \omega)(1-r_i))^2(\eta r_i - \omega)} \right. \\
&\quad \left. + \frac{r_i(c_1 + c_2 + \omega(1-r_i)/r_i)(r_i - (\eta r_i - \omega)(1-r_i))(\eta r_i - \omega) F_2(r_i)}{c_2(r_i - (\eta r_i - \omega)(1-r_i))^2(\eta r_i - \omega)} \right) \\
&= -\frac{\omega(1-c_2)r_i^2}{c_2(\eta r_i^2 - \omega)(\eta r_i - \omega)^3(r_i - (\eta r_i - \omega)(1-r_i))^2} \left((\eta r_i - \omega)^2(1-r_i)(r_i - (\eta r_i - \omega)(1-r_i)) \right. \\
&\quad \left. Q_5(r_i) + r_i \left(\omega(r_i - (\eta r_i - \omega)(1-r_i)) - (c_1 r_i + \omega(1-r_i))(\eta r_i - \omega) \right) F_1(r_i) \right. \\
&\quad \left. + (r_i(c_1 + c_2) + \omega(1-r_i))(\eta r_i - \omega)(r_i - (\eta r_i - \omega)(1-r_i)) F_2(r_i) \right), \tag{34}
\end{aligned}$$

$$\begin{aligned}
J_{k5}(r_i) &= \frac{\omega(1-r_i)}{c_2(r_i - (\eta r_i - \omega)(1-r_i))} Q_4(r_i) \\
&\quad + \frac{-\omega(1-r_i)r_i}{c_2 r_i (\eta r_i - \omega)(1-r_i) - c_2(\eta r_i - \omega)^2(1-r_i)^2} Q_7(r_i) \\
&= \frac{\omega(1-r_i)}{c_2(r_i - (\eta r_i - \omega)(1-r_i))} Q_4(r_i) - \frac{\omega r_i}{c_2(\eta r_i - \omega)(r_i - (\eta r_i - \omega)(1-r_i))} Q_7(r_i). \tag{35}
\end{aligned}$$

These identities follow from the resolvent equation $((1-z)\mathbf{E} - z\mathbf{H})\Phi(z) = \mathbf{I}_{p-k}$, which implies $\mathbf{H}\Phi^2(z) = (1-z)\mathbf{E}\Phi^2(z)/z - \Phi(z)/z$.

Note that the entries of $\mathbf{U}_1^\top \mathbf{W}$ are i.i.d. standard normal and are independent of \mathbf{Y} and $\mathbf{U}_2^\top \mathbf{W}$. Conditional on \mathbf{Y} and $\mathbf{U}_2^\top \mathbf{W}$, we obtain

$$\mathbb{E}(\sqrt{n}[I_{k3}]_{jj}\sqrt{n}[\mathcal{V}_{k1}]_{jj} \mid \mathbf{Y}, \mathbf{U}_2^\top \mathbf{W}) = 0,$$

and similarly

$$\mathbb{E}(\sqrt{n}[I_{k4}]_{jj}\sqrt{n}[\mathcal{V}_{k1}]_{jj} \mid \mathbf{Y}, \mathbf{U}_2^\top \mathbf{W}) = 0.$$

By properties of the standard normal distribution, we also have

$$\mathbb{E}(\sqrt{n}[I_{k3}]_{jj}\sqrt{n}[\mathcal{V}_{k2}]_{jj} \mid \mathbf{Y}, \mathbf{U}_2^\top \mathbf{W}) = \mathbb{E}(\sqrt{n}[I_{k4}]_{jj}\sqrt{n}[\mathcal{V}_{k2}]_{jj} \mid \mathbf{Y}, \mathbf{U}_2^\top \mathbf{W}) = 0.$$

We now justify the derivative estimates, the boundedness of the relevant matrices, and the use of the Poincaré inequality. We begin with the basic deterministic approximation for the resolvent trace. By the cumulant expansion, uniformly for z in a fixed neighborhood of γ_i separated from the limiting spectral support,

$$\mathbb{E} \frac{1}{n} \operatorname{tr} \Phi(z) - QQ_1(z) = O\left(\frac{1}{n}\right).$$

Moreover, by the Gaussian Poincaré inequality,

$$\frac{1}{n} \operatorname{tr} \Phi(z) - \mathbb{E} \frac{1}{n} \operatorname{tr} \Phi(z) = O_p \left(\frac{1}{n} \right).$$

Hence

$$\frac{1}{n} \operatorname{tr} \Phi(z) - QQ_1(z) = O_p \left(\frac{1}{n} \right),$$

uniformly for z in the same neighborhood.

We next explain how derivative estimates are obtained from this approximation. Let $h = m^{-\alpha}$, where $h \downarrow 0$. By the resolvent identity,

$$\frac{\frac{1}{n} \operatorname{tr} \Phi(l_i + h) - \frac{1}{n} \operatorname{tr} \Phi(l_i)}{h} = \frac{1}{n} \operatorname{tr} \left(\Phi(l_i) \mathbf{U}_2^\top \mathbf{W} \mathbf{W}^\top \mathbf{U}_2 \Phi(l_i) \right) + O_p(h).$$

On the other hand, using the deterministic equivalent QQ_1 , we have

$$\begin{aligned} & \frac{\frac{1}{n} \operatorname{tr} \Phi(l_i + h) - \frac{1}{n} \operatorname{tr} \Phi(l_i)}{h} \\ &= \frac{QQ_1(l_i + h) - QQ_1(l_i)}{h} \\ & \quad + \frac{\frac{1}{n} \operatorname{tr} \Phi(l_i + h) - QQ_1(l_i + h) - \left(\frac{1}{n} \operatorname{tr} \Phi(l_i) - QQ_1(l_i) \right)}{h} \\ &= QQ_2(l_i + \xi h) + O_p \left(\frac{1}{nh} \right), \end{aligned}$$

for some $\xi \in (0, 1)$. Since $QQ_2(z)$ is smooth in a neighborhood of γ_i , Taylor expansion gives

$$QQ_2(l_i + \xi h) = QQ_2(l_i) + O_p(h).$$

Therefore,

$$\frac{\frac{1}{n} \operatorname{tr} \Phi(l_i + h) - \frac{1}{n} \operatorname{tr} \Phi(l_i)}{h} = QQ_2(l_i) + O_p(h) + O_p \left(\frac{1}{nh} \right).$$

Choosing $h = n^{-1/2}$ balances the two error terms and yields

$$\frac{\frac{1}{n} \operatorname{tr} \Phi(l_i + n^{-1/2}) - \frac{1}{n} \operatorname{tr} \Phi(l_i)}{n^{-1/2}} = QQ_2(l_i) + O_p(n^{-1/2}).$$

Combining this with the resolvent identity above, we obtain the derivative-type estimate

$$\frac{1}{n} \operatorname{tr} \Phi(l_i) \mathbf{U}_2^\top \mathbf{W} \mathbf{W}^\top \mathbf{U}_2 \Phi(l_i) - QQ_2(l_i) = O_p(n^{-1/2}).$$

The same finite-difference argument will be used repeatedly below. More generally, if a resolvent functional $f_n(z)$ satisfies

$$f_n(z) - f(z) = O_p(n^{-a})$$

uniformly for z in a neighborhood of γ_i , and if the relevant deterministic limit f is smooth with

uniformly bounded derivatives on this neighborhood, then its derivative satisfies

$$f'_n(z) - f'(z) = O_p(n^{-a/2}).$$

Thus each differentiation of a deterministic equivalent may reduce the error exponent by a factor of two. This explains the error orders appearing in the higher-order trace estimates.

We also record the boundedness estimates used throughout the proof. All matrices involved are products of factors such as $\Phi(z)$, \mathbf{E} , \mathbf{H} , $\mathbf{W}\mathbf{W}^\top$, and $\mathbf{Y}\mathbf{Y}^\top$. By the spectral norm inequality,

$$\|\mathbf{A}\mathbf{B}\| \leq \|\mathbf{A}\| \|\mathbf{B}\|,$$

it is enough to control these factors separately. From equation (S3.23) in Bao et al. (2019) [8], for z in the above neighborhood,

$$\|\Phi(z)\| \leq \|(C_{w_2y} - z)^{-1}\| \|S_{w_2w_2}^{-1}\| \leq C$$

with probability tending to one. Moreover, since $\mathbf{W}\mathbf{W}^\top$ and $\mathbf{Y}\mathbf{Y}^\top$ are Gaussian sample covariance matrices, their spectral norms are bounded with probability tending to one. The deterministic matrices \mathbf{E} and \mathbf{H} also satisfy

$$\|\mathbf{E}\| \leq C, \quad \|\mathbf{H}\| \leq C.$$

Consequently, all normalized trace functionals appearing below are uniformly bounded in probability.

Finally, we justify the use of the Poincaré inequality. Let F_n denote any normalized trace functional of the form considered above, for example $F_n = n^{-1} \text{tr} \Phi(z)$, or a normalized trace involving additional bounded factors. Differentiating F_n with respect to the Gaussian entries of \mathbf{W} and \mathbf{Y} produces sums of normalized traces with bounded resolvent factors. Using the uniform spectral norm bounds above, we obtain

$$\sum_{\alpha} \mathbb{E} \left| \frac{\partial F_n}{\partial \xi_{\alpha}} \right|^2 \leq \frac{C}{n^2},$$

where the sum runs over all Gaussian entries involved. Therefore, the Gaussian Poincaré inequality gives

$$\text{Var}(F_n) \leq \frac{C}{n^2}.$$

In particular,

$$F_n - \mathbb{E}F_n = O_p\left(\frac{1}{n}\right).$$

This applies to $n^{-1} \text{tr} \Phi(z)$ and, by the same argument, to all normalized trace quantities used in the cumulant expansion. Hence the products of such normalized traces can be replaced by products of their expectations up to negligible errors by the Cauchy–Schwarz inequality. This completes the proof of Lemma 5.2. \square

7 Proof of Lemma 6.1

We prove (24)–(29) in four parts. Throughout the proof, r_i is fixed and l_i denotes the sample spiked eigenvalue associated with r_i . Since l_i is separated from the limiting bulk, we have

$$l_i - \gamma(r_i) = O_p(n^{-1/2}),$$

where

$$\gamma(r_i) = \frac{r_i - (\eta r_i - \omega)(1 - r_i)}{r_i}.$$

Hence

$$1 - \gamma(r_i) = \frac{(\eta r_i - \omega)(1 - r_i)}{r_i}.$$

We shall also use the identity

$$r_i - (\eta r_i - \omega)(1 - r_i) = ((1 - c_1)r_i + c_1)((1 - c_2)r_i + c_2).$$

First, the deterministic equivalent of $n^{-1} \text{tr} \Phi(l_i)$ is

$$\frac{1}{n} \text{tr} \Phi(l_i) = F_1(r_i) + O_p(n^{-1/2}),$$

where

$$F_1(r_i) = -\frac{c_1 r_i}{((1 - c_1)r_i + c_1)(\eta r_i - \omega)}.$$

Moreover,

$$\frac{1}{n} \text{tr} \mathbf{E} \Phi^2(l_i) = \frac{1}{n} \text{tr} \Phi(l_i) + l_i \left(\frac{1}{n} \text{tr} \Phi(l_i) \right)'$$

Therefore the deterministic equivalent of $QQ_2(l_i)$ is

$$QQ_2(l_i) = F_2(r_i) + O_p(n^{-1/2}),$$

where

$$F_2(r_i) = \frac{r_i^2 (\omega(1 - c_2)r_i((1 - c_1)r_i + c_1) + c_1(\eta r_i - \omega)(\eta r_i^2 - \omega))}{((1 - c_1)r_i + c_1)^2((1 - c_2)r_i + c_2)(\eta r_i - \omega)^2(\eta r_i^2 - \omega)}.$$

With this expression,

$$F_1(r_i) + \gamma(r_i)F_2(r_i) = \frac{\omega(1 - c_2)r_i^2}{(\eta r_i - \omega)^2(\eta r_i^2 - \omega)}.$$

Thus

$$\frac{1}{n} \text{tr} \mathbf{E} \Phi^2(l_i) = \frac{\omega(1 - c_2)r_i^2}{(\eta r_i - \omega)^2(\eta r_i^2 - \omega)} + O_p(n^{-1/2}).$$

We shall also need the derivative of QQ_2 with respect to z . Since

$$\gamma'(r_i) = \frac{\eta r_i^2 - \omega}{r_i^2},$$

the chain rule gives

$$\begin{aligned}
QQ'_2(r_i) &= \frac{r_i^4 (\omega(1-c_2)r_i((1-c_1)r_i+c_1) + c_1(\eta r_i - \omega)(\eta r_i^2 - \omega))}{((1-c_1)r_i+c_1)^2((1-c_2)r_i+c_2)(\eta r_i - \omega)^2(\eta r_i^2 - \omega)^2} \\
&\times \left(\frac{2}{r_i} + \frac{\omega(1-c_2)(2(1-c_1)r_i+c_1) + c_1(\eta(\eta r_i^2 - \omega) + 2\eta r_i(\eta r_i - \omega))}{\omega(1-c_2)r_i((1-c_1)r_i+c_1) + c_1(\eta r_i - \omega)(\eta r_i^2 - \omega)} \right. \\
&\quad \left. - \frac{2(1-c_1)}{(1-c_1)r_i+c_1} - \frac{1-c_2}{(1-c_2)r_i+c_2} - \frac{2\eta}{\eta r_i - \omega} - \frac{2\eta r_i}{\eta r_i^2 - \omega} \right).
\end{aligned}$$

Step 1. Proof of (24). By the cumulant expansion formula, we have

$$\begin{aligned}
\mathbb{E} \frac{1}{n} \operatorname{tr} \mathbf{E} \Phi^2(l_i) &= \frac{q}{n} \mathbb{E} \frac{1}{n} \operatorname{tr} \Phi^2(l_i) \\
&\quad - (1-l_i) \mathbb{E} \left(\frac{1}{n} \operatorname{tr} \mathbf{E} \Phi(l_i) \frac{1}{n} \operatorname{tr} \Phi^2(l_i) + \frac{1}{n} \operatorname{tr} \mathbf{E} \Phi^2(l_i) \frac{1}{n} \operatorname{tr} \Phi(l_i) \right) + O(n^{-1}).
\end{aligned}$$

By the Gaussian Poincaré inequality and the Cauchy–Schwarz inequality, the product terms can be factorized up to negligible errors. Hence

$$\mathbb{E} \frac{1}{n} \operatorname{tr} \Phi^2(l_i) = \frac{1 + (1-l_i) \mathbb{E} \frac{1}{n} \operatorname{tr} \Phi(l_i)}{\frac{1}{n} \operatorname{tr} \mathbf{P}_y - (1-l_i) \mathbb{E} \frac{1}{n} \operatorname{tr} \mathbf{E} \Phi(l_i)} \mathbb{E} \frac{1}{n} \operatorname{tr} \mathbf{E} \Phi^2(l_i) + O(n^{-1}).$$

Substituting the deterministic equivalents above gives

$$\mathbb{E} \frac{1}{n} \operatorname{tr} \Phi^2(l_i) = P_1(r_i) + O(n^{-1/2}),$$

where

$$P_1(r_i) = \frac{c_1(1-c_2)r_i^4}{((1-c_1)r_i+c_1)^2(\eta r_i - \omega)^2(\eta r_i^2 - \omega)}.$$

This proves (24).

Step 2. Proof of (25). Differentiating $n^{-1} \operatorname{tr} \Phi^2(z)$ with respect to z , we obtain

$$\left(\frac{1}{n} \operatorname{tr} \Phi^2(z) \right)' = \frac{2}{nz} (\operatorname{tr} \mathbf{E} \Phi^3(z) - \operatorname{tr} \Phi^2(z)).$$

Therefore, at $z = l_i$,

$$\mathbb{E} \frac{1}{n} \operatorname{tr} \mathbf{E} \Phi^3(l_i) = \mathbb{E} \frac{1}{n} \operatorname{tr} \Phi^2(l_i) + \frac{l_i}{2} \mathbb{E} \left(\frac{1}{n} \operatorname{tr} \Phi^2(l_i) \right)'.$$

Since

$$P_1(r_i) = \frac{c_1(1-c_2)r_i^4}{((1-c_1)r_i+c_1)^2(\eta r_i - \omega)^2(\eta r_i^2 - \omega)},$$

we get

$$\mathbb{E} \left(\frac{1}{n} \operatorname{tr} \Phi^2(l_i) \right)' = P_2(r_i) + O(n^{-1/4}),$$

where

$$P_2(r_i) = \frac{c_1(1-c_2)r_i^6}{((1-c_1)r_i + c_1)^2(\eta r_i - \omega)^2(\eta r_i^2 - \omega)^2} \\ \times \left(\frac{4}{r_i} - \frac{2(1-c_1)}{(1-c_1)r_i + c_1} - \frac{2\eta}{\eta r_i - \omega} - \frac{2\eta r_i}{\eta r_i^2 - \omega} \right).$$

Consequently,

$$\mathbb{E} \frac{1}{n} \operatorname{tr} \mathbf{E} \Phi^3(l_i) = F_3(r_i) + O(n^{-1/4}),$$

where

$$F_3(r_i) = P_1(r_i) + \frac{r_i - (\eta r_i - \omega)(1 - r_i)}{2r_i} P_2(r_i). \quad (36)$$

This proves (25).

For later use, we also record the derivative of QQ_6 . Since $QQ_6(l_i)$ is the deterministic equivalent of

$$\left(\frac{1}{n} \operatorname{tr} \Phi^2(l_i) \right)',$$

we have $QQ_6(l_i) = P_2(r_i) + O_p(n^{-1/4})$. Hence

$$QQ'_6(r_i) = \frac{c_1(1-c_2)r_i^8}{((1-c_1)r_i + c_1)^2(\eta r_i - \omega)^2(\eta r_i^2 - \omega)^3} \\ \times \left(\left(\frac{4}{r_i} - \frac{2(1-c_1)}{(1-c_1)r_i + c_1} - \frac{2\eta}{\eta r_i - \omega} - \frac{2\eta r_i}{\eta r_i^2 - \omega} \right)^2 \right. \\ \left. + \left(\frac{2}{r_i} - \frac{2\eta r_i}{\eta r_i^2 - \omega} \right) \left(\frac{4}{r_i} - \frac{2(1-c_1)}{(1-c_1)r_i + c_1} - \frac{2\eta}{\eta r_i - \omega} - \frac{2\eta r_i}{\eta r_i^2 - \omega} \right) \right. \\ \left. - \frac{4}{r_i^2} + \frac{2(1-c_1)^2}{((1-c_1)r_i + c_1)^2} + \frac{2\eta^2}{(\eta r_i - \omega)^2} + \frac{2\eta(\eta r_i^2 + \omega)}{(\eta r_i^2 - \omega)^2} \right).$$

Step 3. Proof of (26). Applying the cumulant expansion formula to

$$\mathbb{E} \frac{1}{n} \operatorname{tr} \mathbf{E} \Phi^2(l_i) \mathbf{E} \Phi^2(l_i),$$

we obtain

$$\mathbb{E} \frac{1}{n} \operatorname{tr} \mathbf{E} \Phi^2(l_i) \mathbf{E} \Phi^2(l_i) \\ = \mathbb{E} \left(\frac{1}{n} \operatorname{tr} \mathbf{P}_y - \frac{1-l_i}{n} \operatorname{tr} \mathbf{E} \Phi(l_i) \right) \frac{1}{n} \operatorname{tr} \mathbf{E} \Phi^4(l_i) \\ - \mathbb{E} \frac{1-l_i}{n} \operatorname{tr} \mathbf{E} \Phi^2(l_i) \mathbf{E} \Phi^2(l_i) \frac{1}{n} \operatorname{tr} \Phi(l_i) \\ + \mathbb{E} \frac{1}{n} \operatorname{tr} \mathbf{E} \Phi^2(l_i) \left(\frac{1}{n} \operatorname{tr} \Phi^2(l_i) - \frac{1-l_i}{n} \operatorname{tr} \mathbf{E} \Phi^3(l_i) \right) \\ - \mathbb{E} \frac{1-l_i}{n} \operatorname{tr} \mathbf{E} \Phi(l_i) \mathbf{E} \Phi^2(l_i) \frac{1}{n} \operatorname{tr} \Phi^2(l_i) + O(n^{-1}).$$

The Gaussian Poincaré inequality again permits factorization of products of normalized traces, up to negligible errors.

First,

$$\begin{aligned}\mathbb{E}\frac{1}{n}\operatorname{tr}\mathbf{E}\Phi(l_i)\mathbf{E}\Phi^2(l_i) &= F_1(r_i) + 2\frac{r_i - (\eta r_i - \omega)(1 - r_i)}{r_i}F_2(r_i) \\ &\quad + \frac{(r_i - (\eta r_i - \omega)(1 - r_i))^2}{2r_i^2}QQ'_2(r_i) + O(n^{-1/4}).\end{aligned}$$

Second, applying the cumulant expansion formula to

$$\mathbb{E}\frac{1}{n}\operatorname{tr}\mathbf{E}\Phi^3(l_i),$$

we have

$$\mathbb{E}\frac{1}{n}\operatorname{tr}\Phi^3(l_i) = P_3(r_i) + O(n^{-1/8}),$$

where

$$\begin{aligned}P_3(r_i) &= \frac{r_i^2}{c_2((1 - c_1)r_i + c_1)^2}F_3(r_i) \\ &\quad + \frac{(\eta r_i - \omega)(1 - r_i)}{c_2((1 - c_1)r_i + c_1)}P_1(r_i)\frac{\omega(1 - c_2)r_i^2}{(\eta r_i - \omega)^2(\eta r_i^2 - \omega)}.\end{aligned}$$

Differentiating $n^{-1}\operatorname{tr}\Phi^3(z)$ gives

$$\left(\frac{1}{n}\operatorname{tr}\Phi^3(z)\right)' = \frac{3}{nz}(\operatorname{tr}\mathbf{E}\Phi^4(z) - \operatorname{tr}\Phi^3(z)).$$

Thus

$$\mathbb{E}\frac{1}{n}\operatorname{tr}\mathbf{E}\Phi^4(l_i) = \mathbb{E}\frac{1}{n}\operatorname{tr}\Phi^3(l_i) + \frac{l_i}{3}\mathbb{E}\left(\frac{1}{n}\operatorname{tr}\Phi^3(l_i)\right)'.$$

Therefore,

$$\mathbb{E}\frac{1}{n}\operatorname{tr}\mathbf{E}\Phi^4(l_i) = P_3(r_i) + \frac{r_i - (\eta r_i - \omega)(1 - r_i)}{3r_i}P_{3,1}(r_i) + O(n^{-1/16}),$$

where

$$\begin{aligned}P_{3,1}(r_i) &= \frac{2c_1r_i^3}{c_2((1 - c_1)r_i + c_1)^3(\eta r_i^2 - \omega)}F_3(r_i) \\ &\quad + \frac{r_i^2}{c_2((1 - c_1)r_i + c_1)^2}\left(\frac{3}{2}P_2(r_i) + \frac{r_i - (\eta r_i - \omega)(1 - r_i)}{2r_i}QQ'_6(r_i)\right) \\ &\quad + \frac{r_i^2}{\eta r_i^2 - \omega}\left(\frac{\eta(1 - r_i) - (\eta r_i - \omega)}{c_2((1 - c_1)r_i + c_1)} - \frac{(\eta r_i - \omega)(1 - r_i)(1 - c_1)}{c_2((1 - c_1)r_i + c_1)^2}\right) \\ &\quad \quad \times P_1(r_i)\frac{\omega(1 - c_2)r_i^2}{(\eta r_i - \omega)^2(\eta r_i^2 - \omega)} \\ &\quad + \frac{(\eta r_i - \omega)(1 - r_i)}{c_2((1 - c_1)r_i + c_1)} \\ &\quad \times \left(P_2(r_i)\frac{\omega(1 - c_2)r_i^2}{(\eta r_i - \omega)^2(\eta r_i^2 - \omega)} + P_1(r_i)\left(2F_2(r_i) + \frac{r_i - (\eta r_i - \omega)(1 - r_i)}{r_i}QQ'_2(r_i)\right)\right).\end{aligned}$$

Substituting these estimates into the cumulant expansion above yields

$$\mathbb{E} \frac{1}{n} \operatorname{tr} \mathbf{E} \Phi^2(l_i) \mathbf{E} \Phi^2(l_i) = Q_3(r_i) + O(n^{-1/16}),$$

where

$$\begin{aligned} Q_3(r_i) = & \frac{c_2((1-c_1)r_i + c_1)^2}{r_i^2} \left(P_3(r_i) + \frac{r_i - (\eta r_i - \omega)(1-r_i)}{3r_i} P_{3,1}(r_i) \right) \\ & - \frac{(1-c_1)r_i + c_1}{r_i} \left(P_1(r_i) - \frac{(\eta r_i - \omega)(1-r_i)}{r_i} F_3(r_i) \right) \frac{\omega(1-c_2)r_i^2}{(\eta r_i - \omega)^2(\eta r_i^2 - \omega)} \\ & - \frac{((1-c_1)r_i + c_1)(\eta r_i - \omega)(1-r_i)}{r_i^2} P_1(r_i) \\ & \times \left(F_1(r_i) + 2 \frac{r_i - (\eta r_i - \omega)(1-r_i)}{r_i} F_2(r_i) + \frac{(r_i - (\eta r_i - \omega)(1-r_i))^2}{2r_i^2} Q Q'_2(r_i) \right). \end{aligned} \quad (37)$$

This proves (26).

Step 4. Proof of (27)–(29). First, we prove (27). Applying the cumulant expansion formula to the Y -entries gives

$$\begin{aligned} & \mathbb{E} \frac{1}{n} \operatorname{tr} \mathbf{Y} \mathbf{W}^\top \mathbf{U}_2 \Phi^2(l_i) \mathbf{E} \Phi^2(l_i) \mathbf{U}_2^\top \mathbf{W} \mathbf{Y}^\top \\ = & \mathbb{E} \left(c_2 - \frac{1}{n} \operatorname{tr} \mathbf{H} \Phi(l_i) \right) \frac{1}{n} \operatorname{tr} \mathbf{E} \Phi^2(l_i) \mathbf{E} \Phi^2(l_i) \\ & + \mathbb{E} \left(c_2 - \frac{1}{n} \operatorname{tr} \mathbf{E} \Phi(l_i) \right) \frac{1}{n} \operatorname{tr} \mathbf{H} \Phi^2(l_i) \mathbf{E} \Phi^2(l_i) \\ & + \mathbb{E} \frac{1}{n} \operatorname{tr} \mathbf{H} \Phi^2(l_i) \frac{1}{n} \operatorname{tr} \mathbf{E} \Phi^2(l_i) \\ & - \mathbb{E} \frac{1}{n} \operatorname{tr} \mathbf{E} \Phi^2(l_i) \frac{1}{n} \operatorname{tr} \mathbf{E} \Phi(l_i) \mathbf{H} \Phi^2(l_i) \\ & - \mathbb{E} \frac{1}{n} \operatorname{tr} \mathbf{H} \Phi^2(l_i) \frac{1}{n} \operatorname{tr} \mathbf{E} \Phi(l_i) \mathbf{E} \Phi^2(l_i) + O(n^{-1}). \end{aligned}$$

Using

$$\mathbf{H} \Phi^2(l_i) = \frac{1-l_i}{l_i} \mathbf{E} \Phi^2(l_i) - \frac{1}{l_i} \Phi(l_i),$$

and substituting the estimates proved above, we obtain

$$\mathbb{E} \frac{1}{q} \operatorname{tr} \mathbf{Y} \mathbf{W}^\top \mathbf{U}_2 \Phi^2(l_i) \mathbf{E} \Phi^2(l_i) \mathbf{U}_2^\top \mathbf{W} \mathbf{Y}^\top = \frac{Q_4(r_i)}{c_2} + O(n^{-1/16}),$$

where

$$\begin{aligned} Q_4(r_i) = & \frac{(c_1 + c_2)r_i + 2\omega(1-r_i)}{r_i - (\eta r_i - \omega)(1-r_i)} Q_3(r_i) \\ & - \frac{r_i(c_2(\eta r_i - \omega) + \omega)}{(\eta r_i - \omega)(r_i - (\eta r_i - \omega)(1-r_i))} P_3(r_i) \end{aligned} \quad (38)$$

$$\begin{aligned}
& - \frac{\omega(1-c_2)r_i(r_i - (\eta r_i - \omega)(1-r_i))}{(\eta r_i - \omega)^2(\eta r_i^2 - \omega)} F_3(r_i) \\
& + \frac{(c_1 r_i + \omega(1-r_i))(\eta r_i - \omega)(\eta r_i^2 - \omega) + \omega(1-c_2)r_i^2(1-r_i)}{(\eta r_i - \omega)(\eta r_i^2 - \omega)(r_i - (\eta r_i - \omega)(1-r_i))} Q Q'_2(r_i) \\
& + \frac{\omega(1-c_2)c_1 r_i^4}{(\eta r_i - \omega)^2(\eta r_i^2 - \omega)^2((1-c_1)r_i + c_1)^2} \\
& + \frac{\omega(1-c_2)r_i^2(c_1 r_i + \omega(1-r_i))}{(\eta r_i - \omega)^2(\eta r_i^2 - \omega)(r_i - (\eta r_i - \omega)(1-r_i))} \\
& + \frac{\omega^2(1-c_2)^2 r_i^4(1-r_i)}{(\eta r_i - \omega)^3(\eta r_i^2 - \omega)^2(r_i - (\eta r_i - \omega)(1-r_i))}.
\end{aligned}$$

This proves (27).

Next, we prove (28). Applying the same cumulant expansion argument to

$$\mathbb{E} \frac{1}{q} \text{tr} \mathbf{Y} \mathbf{W}^\top \mathbf{U}_2 \Phi^2(l_i) \mathbf{E} \Phi(l_i) \mathbf{U}_2^\top \mathbf{W} \mathbf{Y}^\top$$

and using the same resolvent identity, we get

$$\mathbb{E} \frac{1}{q} \text{tr} \mathbf{Y} \mathbf{W}^\top \mathbf{U}_2 \Phi^2(l_i) \mathbf{E} \Phi(l_i) \mathbf{U}_2^\top \mathbf{W} \mathbf{Y}^\top = \frac{Q_5(r_i)}{c_2} + O(n^{-1/4}),$$

where

$$\begin{aligned}
Q_5(r_i) &= \left(c_2 + \frac{c_1 r_i + \omega(1-r_i)}{r_i - (\eta r_i - \omega)(1-r_i)} \right) \left(\frac{\omega(1-c_2)r_i^2}{(\eta r_i - \omega)^2(\eta r_i^2 - \omega)} + Q Q'_2(r_i) \right) \\
& - \frac{c_1 \omega \eta r_i^4}{((1-c_1)r_i + c_1)^2 (\eta r_i - \omega)^2 (\eta r_i^2 - \omega)^2} \\
& + \left(c_2 + \frac{\omega}{\eta r_i - \omega} \right) \left(\frac{(\eta r_i - \omega)(1-r_i)}{r_i - (\eta r_i - \omega)(1-r_i)} - \frac{r_i - (\eta r_i - \omega)(1-r_i)}{r_i} \right) \\
& \quad \times \left(\frac{\omega(1-c_2)r_i^2}{(\eta r_i - \omega)^2(\eta r_i^2 - \omega)} + Q Q'_2(r_i) \right).
\end{aligned} \tag{39}$$

Here we used the simplification

$$\begin{aligned}
& \frac{\eta \omega r_i^2}{(\eta r_i^2 - \omega)(\eta r_i - \omega)^2} - \frac{\eta \omega(1-r_i)r_i}{(\eta r_i^2 - \omega)(\eta r_i - \omega)} - \frac{\omega}{\eta r_i - \omega} + \frac{\omega}{\eta r_i^2 - \omega} \\
& = \frac{\omega \eta r_i^2}{(\eta r_i - \omega)^2(\eta r_i^2 - \omega)}.
\end{aligned}$$

This proves (28).

Finally, we prove (29). Applying the cumulant expansion formula to

$$\mathbb{E} \frac{1}{q} \text{tr} \mathbf{Y} \mathbf{W}^\top \mathbf{U}_2 \Phi^3(l_i) \mathbf{U}_2^\top \mathbf{W} \mathbf{Y}^\top$$

and using

$$\mathbf{H}\Phi^3(l_i) = \frac{1-l_i}{l_i}\mathbf{E}\Phi^3(l_i) - \frac{1}{l_i}\Phi^2(l_i),$$

we obtain

$$\mathbb{E}\frac{1}{q}\text{tr}\mathbf{Y}\mathbf{W}^\top\mathbf{U}_2\Phi^3(l_i)\mathbf{U}_2^\top\mathbf{W}\mathbf{Y}^\top = \frac{Q_7(r_i)}{c_2} + O(n^{-1/8}),$$

where

$$\begin{aligned} Q_7(r_i) = & \left(c_2 + \frac{\omega}{\eta r_i - \omega} \right) \left(\frac{(\eta r_i - \omega)(1-r_i)}{r_i - (\eta r_i - \omega)(1-r_i)} F_3(r_i) \right. \\ & - \frac{r_i^2(2r_i P_1(r_i) + r_i - (\eta r_i - \omega)P_2(r_i))}{2((1-c_1)r_i + c_1)(r_i - (\eta r_i - \omega)(1-r_i))(c_2 r_i - \omega(1-r_i))} \\ & \left. + \frac{\omega(1-c_2)(1-r_i)r_i^3 P_1(r_i)}{(\eta r_i - \omega)(\eta r_i^2 - \omega)(r_i - (\eta r_i - \omega)(1-r_i))(c_2 r_i - \omega(1-r_i))} \right) \\ & - \frac{\omega(1-c_2)c_1 r_i^4}{(\eta r_i - \omega)^2(\eta r_i^2 - \omega)^2((1-c_1)r_i + c_1)^2} \\ & + \left(c_1 + c_2 + \frac{\omega(1-r_i)}{r_i} \right) F_3(r_i). \end{aligned} \quad (40)$$

In the last simplification, we used

$$r_i + (\eta r_i - \omega)(1-r_i)F_1(r_i) = \frac{r_i^2}{(1-c_1)r_i + c_1}.$$

This proves (29).

Combining (24)–(29), Lemma 6.1 follows.

8 Proofs of Proposition 3.1 and Proposition 3.3

Proof of Proposition 3.1. By Theorem 1.4, we have

$$l_i \xrightarrow{P} \gamma(r_i).$$

Since $\gamma(\cdot)$ is locally one-to-one in a neighborhood of r_i , and $\gamma^{-1}(\cdot)$ denotes the corresponding local inverse, there exists a neighborhood U of r_i such that γ is one-to-one on U . Let $V = \gamma(U)$ be the corresponding neighborhood of $\gamma(r_i)$ on which the local inverse γ^{-1} is well defined. Since γ is continuous in the present setting, the local inverse γ^{-1} is continuous at $\gamma(r_i)$.

We now show that $\hat{r}_i \rightarrow r_i$ in probability. Let $\epsilon > 0$, since γ^{-1} is continuous at $\gamma(r_i)$, there exists $\delta > 0$ such that

$$|x - \gamma(r_i)| < \delta \quad \Rightarrow \quad |\gamma^{-1}(x) - r_i| < \epsilon.$$

Consequently,

$$\{|\hat{r}_i - r_i| \geq \epsilon\} \subset \{|l_i - \gamma(r_i)| \geq \delta\},$$

and hence

$$\mathbb{P}(|\hat{r}_i - r_i| \geq \epsilon) \leq \mathbb{P}(|l_i - \gamma(r_i)| \geq \delta) \rightarrow 0.$$

Therefore,

$$\hat{r}_i \xrightarrow{p} r_i.$$

Next, by assumption, $d(\cdot)$ is continuous at r_i . Hence, by the continuous mapping theorem,

$$d(\hat{r}_i) \xrightarrow{p} d(r_i).$$

Since the function $x \mapsto 1/(1+x)$ is continuous at $d(r_i)$. Applying the continuous mapping theorem again yields

$$\hat{\mu}_i = \frac{1}{1+d(\hat{r}_i)} \xrightarrow{p} \frac{1}{1+d(r_i)} = \mu_i.$$

This proves

$$\hat{r}_i \xrightarrow{p} r_i, \quad \hat{\mu}_i \xrightarrow{p} \mu_i.$$

□

Proof of Proposition 3.3. By Proposition 3.1, $\hat{r}_i \xrightarrow{p} r_i$. Since $d(\cdot)$ and $\sigma^2(\cdot)$ are continuous at r_i , the continuous mapping theorem yields

$$d(\hat{r}_i) \xrightarrow{p} d(r_i), \quad \sigma^2(\hat{r}_i) \xrightarrow{p} \sigma^2(r_i).$$

Moreover, $1+d(r_i) \neq 0$. Hence,

$$\hat{\tau}_i^2 = \frac{\sigma^2(\hat{r}_i)}{(1+d(\hat{r}_i))^4} \xrightarrow{p} \frac{\sigma^2(r_i)}{(1+d(r_i))^4} = \tau_i^2.$$

Since $0 < \sigma^2(r_i) < \infty$, we have $0 < \tau_i^2 < \infty$. Therefore, by the continuity of $x \mapsto \sqrt{x}$ on $(0, \infty)$,

$$\hat{\tau}_i = \sqrt{\hat{\tau}_i^2} \xrightarrow{p} \sqrt{\tau_i^2} = \tau_i.$$

This proves the proposition. □

Acknowledgments

The authors would like to thank Zhigang Bao for many illuminating discussions in an early stage of this research.

funding

Xiaozhuo Zhang was partially supported by NSFC Grants No. 12401338, the Science Research Project of the Education Department of Jilin Province Grant No. JJKH20261178KJ.

Jiang Hu was partially supported by NSFC Grants No. 12571280, Science and Technology Development Plan Project of Jilin Province, China, No. 20260101010JJ.

References

- [1] Anderson, T. W. (2003). *An introduction to multivariate statistical analysis*, volume 3. Wiley New York.
- [2] Bai, Z. and feng Yao, J. (2008). Central limit theorems for eigenvalues in a spiked population model. *Annales de l'Institut Henri Poincaré, Probabilités et Statistiques*, 44(3):447 – 474.
- [3] Bai, Z., Hou, Z., Hu, J., Jiang, D., and Zhang, X. (2022). Limiting canonical distribution of two large-dimensional random vectors. In *Methodology and Applications of Statistics: A Volume in Honor of CR Rao on the Occasion of his 100th Birthday*, pages 213–238. Springer.
- [4] Bai, Z., Miao, B., and Pan, G. (2007). On asymptotics of eigenvectors of large sample covariance matrix. *The Annals of Probability*, 35(4):1532–1572.
- [5] Bai, Z. D. and Silverstein, J. W. (2004). CLT for linear spectral statistics of large-dimensional sample covariance matrices. *The Annals of Probability*, 32(1A):553 – 605.
- [6] Bao, Z., Ding, X., Wang, J., and Wang, K. (2022). Statistical inference for principal components of spiked covariance matrices. *The Annals of Statistics*, 50(2):1144–1169.
- [7] Bao, Z., Ding, X., and Wang, K. (2021). Singular vector and singular subspace distribution for the matrix denoising model. *Ann. Statist.*, 49(1):370–392.
- [8] Bao, Z., Hu, J., Pan, G., and Zhou, W. (2019). Canonical correlation coefficients of high-dimensional gaussian vectors: Finite rank case. *The Annals of Statistics*, 47(1):612–640.
- [9] Bao, Z., Wang, D., and Zhu, Y. (2026). Eigenvector distribution of random matrices under critical finite-rank deformations.
- [10] Bykhovskaya, A. and Gorin, V. (2023). High-dimensional canonical correlation analysis. *arXiv preprint arXiv:2306.16393*.
- [11] Fan, J., Fan, Y., Han, X., and Lv, J. (2022). Asymptotic theory of eigenvectors for random matrices with diverging spikes. *Journal of the American Statistical Association*, 117(538):996–1009.
- [12] Gittins, R. (1985). *Canonical Analysis: A Review with Applications in Ecology*, volume 12 of *Biomathematics*. Springer, Berlin, Heidelberg.
- [13] Harold, H. (1936). Relations between two sets of variables. *Biometrika*, 28(3):321–377.
- [14] Hotelling, H. (1935). The most predictable criterion. *Journal of educational Psychology*, 26(2):139.
- [15] Hou, Z., Zhang, X., Bai, Z., and Hu, J. (2023). Spiked eigenvalues of noncentral fisher matrix with applications. *Bernoulli*, 29(4):3171–3197.
- [16] Lei, J. (2016). A goodness-of-fit test for stochastic block models. *The Annals of Statistics*, 44(1):401–424.

- [17] Li, Y., Zhou, H., and Hu, J. (2023). The eigenvector lsd of information plus noise matrices and its application to linear regression model. *Statistics & Probability Letters*, 197:109811.
- [18] Liu, X., Liu, Y., Pan, G., Zhang, L., and Zhang, Z. (2023). Asymptotic properties of spiked eigenvalues and eigenvectors of signal-plus-noise matrices with their applications. *arXiv preprint arXiv:2310.13939*.
- [19] Lytova, A. and Pastur, L. (2009). Central limit theorem for linear eigenvalue statistics of random matrices with independent entries. *The Annals of Probability*, 37(5):1778 – 1840.
- [20] Ma, Z. and Yang, F. (2023). Sample canonical correlation coefficients of high-dimensional random vectors with finite rank correlations. *Bernoulli*, 29(3):1905–1932.
- [21] Muirhead, R. J. (1982). *Aspects of multivariate statistical theory*. John Wiley & Sons.
- [22] Paul, D. (2007). Asymptotics of sample eigenstructure for a large dimensional spiked covariance model. *Statist. Sinica*, 17(4):1617–1642.
- [23] Pu, Z., Zhang, X., Hu, J., and Bai, Z. (2024). The asymptotic properties of the extreme eigenvectors of high-dimensional generalized spiked covariance model. *arXiv preprint arXiv:2405.08524*.
- [24] Wachter, K. W. (1980). The Limiting Empirical Measure of Multiple Discriminant Ratios. *The Annals of Statistics*, 8(5):937 – 957.
- [25] Xi, H., Yang, F., and Yin, J. (2020). Convergence of eigenvector empirical spectral distribution of sample covariance matrices. *The Annals of Statistics*, 48(2):953–982.
- [26] Xia, N., Qin, Y., and Bai, Z. (2013). Convergence rates of eigenvector empirical spectral distribution of large dimensional sample covariance matrix. *The Annals of Statistics*, 41(5):2572–2607.
- [27] Yang, F. (2022). Limiting distribution of the sample canonical correlation coefficients of high-dimensional random vectors. *Electronic Journal of Probability*, 27:1–71.
- [28] Yang, Y. and Pan, G. (2012). The convergence of the empirical distribution of canonical correlation coefficients. *Electronic Journal of Probability*, 17:1–13.
- [29] Yang, Y. and Pan, G. (2015). Independence test for high dimensional data based on regularized canonical correlation coefficients. *The Annals of Statistics*, 43(2):467–500.
- [30] Zhang, X. (2023). The limiting spectral distribution of the sample canonical correlation matrix. *arXiv preprint arXiv:2309.13369*.